which is coencapsulated in the vesicles (*27*, *28*). As a result, the functional half-life of the Hb-vesicles is doubled by coencapsulation of the DL-homocysteine and active oxygen scavengers (*27*, *29*). To retard metHb formation, bioconjugation of enzymes such as catalase or superoxide dismutase (SOD) (*30*) and coencapsulation of RBC enzymes including the metHb reductase system, carbonic anhydrase, SOD, or catalase (*29*, *31*) have also been reported.

To restore the O_2 binding property of HbV, we tested utilization of the photoreduction system: the indirect excitation of an externally added electron mediator (*32*), or the direct excitation of metHb absorption in the UV region (*7*). In this study, we have made significant efforts to find out a condition that facilitates metHb reduction by a photoreduced flavin mononucleotide (FMN), because this system was well characterized by Everse (*32*), and the advantages of this system are visible light irradiation and high quantum yield (*9*, *10*). We analyzed the influence of electron donors to FMN, dissolved gases, etc., to find the facilitating condition and elucidate the mechanism for the facilitation of the metHb photoreduction in the HbV nanoparticles, a structure similar to that in red blood cells (RBCs), and this may also help understand the underlying mechanism of the reaction of NADPH-flavin reductase and metHb in RBCs.

EXPERIMENTAL PROCEDURES

Preparation of metHb. Carbonylhemoglobin (HbCO) was purified from outdated donated blood offered by the Hokkaido Red Cross Blood Center as previously reported (*33*, *34*). MetHb was prepared by reacting HbCO with an excess amount of potassium ferricyanide. The unreacted ions and ferrocyanide ions were removed twice by stirring with a mixed bed ion-exchange resin (Bio Rad AG 501-X8), and the solution was then permeated through 0.22 μm-filters (Advantec Co.). The metHb conversion was 99.8% measured by the cyanomethemoglobin method.

Chemicals. Amino acids (Met, Gln, Arg, Glu, Phe, Lys, Tyr, and Trp) were purchased from the Kanto Chem. Co (Tokyo). Peptides (Met-Met and Met-Gly) were from Sigma, and saccharides (mannitol, maltotriose, dextran, glucoseamine, glucron amide), methanol, citric acid sodium salt, ethylenediamine tetraacetic acid (EDTA), and diethylenetriamine pentaacetic acid (DTPA) were from the Kanto Chem. Co. All the chemicals were used without purification.

Photoreduction of FMN in the Presence of an Electron Donor. Three milliliters of phosphate-buffered saline (10 mM PBS, pH 7.4) with an electron donor (e.g., amino acids, peptides, sugars, as listed above, 20 mM) was sealed in a cuvette (2 mm width) with a butyl rubber cap. The solution was bubbled with N_2 for 30 min. A stock solution of FMN prepared in the dark was added at a concentration of 10 μM. The light source was a super high-pressure mercury lamp (USH-250D, 250W, Ushio Co., Tokyo) with a cutoff filter (L-42 and HA-50, Hoya Co., Tokyo) to obtain a single beam with the maximum wavelength of about 435 nm, which is close to λ_{max} of FMN (450 nm). The cuvette was located 2.5 cm away from the light source, and the light intensity was 221 mW/cm^2 that was measured with a power meter (PSV-3102, Gentec Co.). The conversion of the reduction, FMN to $FMNH_2$, was calculated from the reduction of absorbance at 450 nm, measured with an UV/vis spectrophotometer (V-560, Jasco, Tokyo).

Photoreduction of metHb in the Presence of FMN and an Electron Donor. Three milliliters of phosphate-buffered saline (10 mM PBS, pH 7.4) with an electron donor and FMN was sealed in a cuvette (2 mm width) with a butyl rubber cap. The solution was bubbled with N_2 gas for 30 min. A concentrated metHb stock solution deaerated by a gentle N_2 flowing in another bottle (about 3 mM, 10 μL) was injected into the cuvette. This procedure avoided bubbling of a metHb solution that might induce foaming and metHb denaturation. The final concentration of heme was 0.1 mM. The cuvette was exposed to the same visible light (435 nm) as described above. The conversion of the metHb reduction was calculated from the ratio of the Soret band absorption at 405 nm (λ_{max} of metHb) versus 430 nm (deoxyHb) or 415 nm (HbO_2).

A laser flash photolysis system (Tokyo Instr. Co.) was used for the transient spectrum measurement of the reduction of FMN and the succeeding metHb (*7*). The sample solutions were excited at 450 nm with a Pulsed Nd:YAG laser (SL803G-10, Spectron Laser Systems, Ltd.) equipped with an optical parametric oscillator. One irradiation time was 5−8 ns (fwhm) and the interval was 100 ms. A total of 100 accumulations were collected to get an acceptable signal-to-noise ratio. The transient spectra were recorded between 350 and 550 nm using a spectrophotometer (MS257, Oliel Instr. Co.) equipped with an ICCD detector (DH520−18F−WR, ANDOR Technol. Co.). A sample solution was placed in a 10 mm quartz cuvette and purged with N_2. The fastest time point of the measurements was 30 ns. A solution of FMN (100 μM)/Met (20 mM) in a 10 mM phosphate-buffered saline (pH 7.4), and a solution of FMN (5 μM)/Met (20 mM)/metHb ([heme] = 10 μM) in the phosphate-buffered saline were tested.

Quantum Yield Measurement. The ferroioxalate actinometer of $K_3[Fe(C_2O_4)_3]\cdot 3H_2O$ was used to measure the quantum yield (Φ) of metHb photoreduction (*7*, *35*, *36*). In the actinometer, Φ of the photoreduction of Fe^{3+} to Fe^{2+} was assumed to be 1.11 (*35*), and this value was used to calculate the total photons absorbed by the sample solution and Φ of the metHb photoreductions.

Isoelectric Focusing (IEF) and Native Polyacrylaminde Gel Electrophoresis (Native-PAGE). IEF and native-PAGE were performed on PhastGel IEF 3−9 (pH 3−9) and PhastGel Gradient 8−25 (PAGE content, 8−25%) (Amersham Pharmacia Biotech), respectively, with the PhastSystem (Pharmacia). The photoreduced Hbs in N_2 and air in the presence of FMN/EDTA was compared with metHb and the purified HbO_2.

IEF. Forty microliters of sample (1 mg/mL) per one lane was applied on the gel. This was focused and then stained with PhastGel Blue R (Coomassie brilliant blue) in the development unit of the PhastSystem. The marker was the p*I* calibration kit 3−10 (Pharmacia).

Native-PAGE. The samples were applied on the gel and the electrophoresis was automatically performed. The gel was stained with PhastGel Blue R. The marker was HMW Kit E (Parmacia).

Restoration of Oxygen Binding Property. The photoreduced deoxyHb solution ([heme] = 20 mM, [FMN] = 5 μM, [EDTA] = 10 mM) in an Ar atmosphere was bubbled with oxygen, and the UV/vis spectroscopy was measured. The photoreduced Hb solution was permeated through a column of Sephadex G-25 (Pharmacia) to remove FMN, the oxygen equilibrium curve of the obtained Hb solution was obtained at 37 °C with a Hemox Analyzer (TCS Products Inc.), and the oxygen affinity (P_{50}) and Hill number were measured. The Hb samples were diluted in a Hemox phosphate buffer (TCS Products Inc.).

Preparation of Hb-Vesicles Coencapsulating FMN and EDTA, and the Photoreduction of metHb. HbVs were prepared as previously reported (*24, 34, 37*). The purified HbO_2 solution (35 g/dL, [heme] = 21.7 mM) contained FMN (5, 10, or 50 mM) and EDTA (10, 20, 30, 50, or 200 mM), this was mixed with the lipid mixtures, and the resulting multilamellar vesicles were extruded through filters to regulate the vesicular size. The lipid bilayer was composed of a mixture of 1,2-dipalmitoyl-*sn*-glycero-3-phosphatidylcholine (DPPC), cholesterol, and 1,5-*O*-dihexadecyl-*N*-succinyl-L-glutamate (DHSG) at the molar ratio of 5/5/1 (Nippon Fine Chem. Co., Osaka), and 1,2-distearoyl-*sn*-glycero-3-phosphatidylethanolamine-*N*-PEG_{5000} (PEG-DSPE, NOF Co., Tokyo) (*38*). Thus the vesicular surface was covered with PEG chains. The molar composition of the DPPC/cholesterol/DHSG/PEG-DSPE was 5/5/1/0.033. HbVs were suspended in a physiologic salt solution at [Hb] = 10 g/dL. The suspension was incubated in the dark at 40 °C for 48 h to facilitate the metHb formation and to prepare metHbV. The concentrations of FMN, EDTA, and heme of Hb in HbV, expressed as $[FMN]_{in}$, $[EDTA]_{in}$, and $[heme]_{in}$, respectively, are assumed to be identical to the fed concentrations for the HbV preparation.

Photoreduction of metHbV was performed in the same manner with a metHb solution in a relatively diluted condition ([heme] = 10 μM) in a 2 mm quartz cuvette. At a higher concentration ([heme] = 5 mM) under aerobic condition, the suspension of metHbV was sandwiched between two glass plates. The optical path length was 10 μm.

Measurement of H_2O_2 in the metHb Photoreduction. The reaction of *p*-hydroxyphenyl acetic acid (PHA) and H_2O_2 to generate a fluorescent dimer, 6,6′-dihydroxy (1,1′-biphenyl)-3,3′-diacetic acid (DBDA), was used to detect H_2O_2 generated during the metHb photoreduction in the metHbV and metHb solutions. During the photoreduction of metHb or metHbV ([heme] = 20 μM in a cuvette) in the presence of FMN (5 μM)/EDTA (50 μM), 1 mL of sample was pipetted out and immediately mixed with horseradish peroxidase (Sigma, 3.7 μM), and PHA (5.8 mM). The mixture was ultracentrifuged in a tube with a filter (Cut off Mw. 30 kDa, Ultrafree, Amicon) at 12 000 rpm for 20 min to remove Hb or HbV and to obtain the filtrate solution. The fluorescence of the filtrate was measured with a fluorometer (JASCO, Ex: 317 nm, Em: 404 nm). The calibration curve was obtained by analysis of a diluted standard H_2O_2 solution (Kanto Chem., Co).

RESULTS

Photoreduction of FMN with an Electron Donor. Figure 1 shows the time course of the conversion of FMN to $FMNH_2$ by irradiation of visible light (435 nm). FMN primarily converts to the photoexcited triplet FMN* and this reacts with two electron donors (D) to generate $FMNH_2$. The reduction can be confirmed by the decrease in the absorption of the characteristics peaks at 370 and 450 nm. Without an addition of an electron donor, photoreduction gradually proceeds (baseline, initial reduction rate = 12 μM/min) (Table 1). A ribityl group in a FMN molecule of itself can be an electron donor. However, further irradiation should induce decomposition that was evident from the phenomena that the spectroscopic curves did not coincide at the isosbestic point. A significantly fast reduction was observed by the addition of EDTA and DTPA that were 88 and 84 times faster than the condition without the addition of an electron donor. Among the amino acids, Met showed the fastest

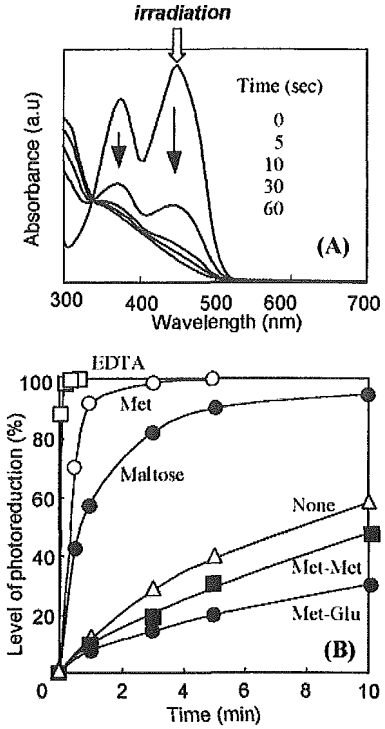

Figure 1. (A) Time course of the spectral changes during the conversion of FMN to $FMNH_2$ in the presence of EDTA (20 mM) by visible light irradiation (435 nm). The characteristic two peaks disappeared with the photoreduction conversion. (B) Time course of the conversion of FMN to $FMNH_2$ with various electron donors. EDTA and Met showed fast photoreduction rate. On the other hand, Met-Met and Met-Glu retarded the reaction. [FMN] = 100 μM, [electron donor] = 20 mM, pH = 7.4, in N_2 atmosphere.

Table 1. Initial Rates of the Photoreduction of FMN to $FMNH_2$ with Various Electron Donors (10 mM)

electron donor	mw	initial reduction rate (μM/min)	comparison with baseline
EDTA	292	1056	88
DTPA	393	1008	84
Met	149	140	11.7
Met-Met (10 mM)	280	5	0.2
Met-Met (20 mM)	280	10	0.8
Met-Glu	278	7	0.6
Arg	174	124	10.3
Phe	165	118	9.8
Lys	146	104	8.7
Gln	146	58	4.8
Glu	147	46	3.8
mannitol	182	45	3.8
maltotriose (10 unit mM)	504	47	3.9
dextran (10 unit mM)	5×10^6	45	3.6
glucoseamine	216	100	8.3
glucron amide	193	72	6.0
methanol	32	42	3.5
citric acid sodium salt	294	40	3.3
hydrogen	2	82	6.8
none (baseline)	---	12	1.0

reduction rate (140 μM/min, 12 times faster than the baseline), while Arg, Phe, Lys, Glu, and Gln showed moderate facilitation. On the other hand, Tyr and Trp showed slower rates of photoreduction. Unexpectedly, Met-Met and Met-Glu lowered the reduction rate. As for the saccharides, mannitol, maltotriose, dextran, glucosamine, and glucron amide showed similar facilitation at the same glucose units. However, they are much slower than Met and EDTA. The presence of H_2 gas

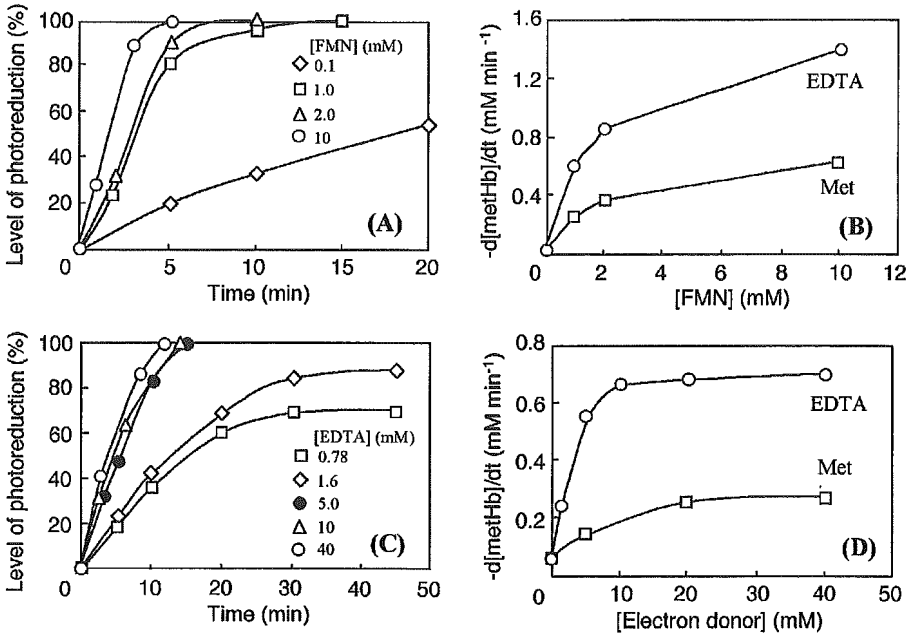

Figure 2. Influence of the concentrations of FMN and EDTA on the rate of metHb reduction. The time course of the level of photoreduction and the initial reaction rates are summarized. (A, B): Influence of the FMN concentration at a constant [EDTA] (20 mM). [FMN] was at 0.1, 1.0, 2.0, or 10 mM. (C, D): Influence of [EDTA] at the constant [FMN] (1.0 mM). [EDTA] was at 0.78, 1.6, 5.0, 10, or 40 mM. The data for the Met addition were inserted as a reference. [heme] = 3.1 mM.

slightly facilitated the reduction. Citric acid and methanol showed a slight facilitation. From these results, EDTA and Met were mainly studied as electron donors.

Reduction of metHb by the Photoreduced FMNH$_2$. The reduction of metHb by the photoreduced FMNH$_2$ was evident from the spectroscopic change of λ_{max} in the Soret and Q-bands. The influence of the concentration of FMN was examined at constant concentrations of metHb (5 g/dL, [heme] = 3.1 mM) and EDTA (20 mM) (Figure 2A). The presence of 100 μM FMN showed 50% reduction of metHb at 20 min; however, 1 mM FMN completed the reduction at 15 min. The influence of the EDTA concentration was examined at constant concentrations of metHb ([heme] = 3.1 mM) and FMN (1.0 mM) (Figure 2B). Without EDTA, the metHb photoreduction proceeded since a ribityl group of FMN and probably globin of Hb can be an electron donor. When the EDTA concentration was less than that of the heme concentration, the reduction rate was very slow, and the reduction could not be completed. However, 5 mM EDTA and higher showed a faster rate and the reduction was completed within 15 min. Similar results were obtained with Met; however, the initial rates were much slower than with EDTA.

The transient spectrum of the photoreduction of FMN in the presence of Met after laser flash irradiation showed the reduction of the absorbances at 445 and 373 nm at 30 ns, and the spectral profile was the same at 5 ms (data not shown here). Therefore, the photoreduction of FMN to FMNH$_2$ was completed within 30 ns. In the presence of metHb, a total of 30 ns was enough to observe the reduced deoxyHb (λ_{max} = 430 nm) and the spectrum was the same for 5 ms.

The influence of the presence of O_2 was examined (Figure 3). The metHb photoreduction in the presence of EDTA and FMN in the N_2 atmosphere completed the reduction within 15 min. The metHb photoreduction under the aerobic conditions became slightly slower, and the level of reduction reached 95% and then showed a plateau. In the case of the addition of Met, the reduction was completed within 40 min in the N_2 atmosphere that

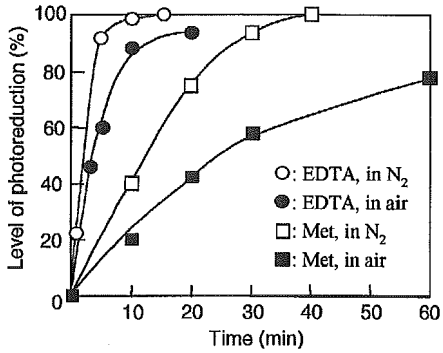

Figure 3. The influence of the presence of O_2 on the rate of photoreduction of metHb ([heme] = 3.1 mM) with FMN (1.0 mM) and an electron donor (20 mM) at pH 7.4. The data for Met addition (1.0 mM) were also inserted as a reference. The presence of O_2 retarded the metHb photoreduction.

was much slower in comparison with the EDTA addition. Under the aerobic condition, the reduction in the presence of Met was significantly slow and did not reach 80% at 60 min.

Native-PAGE of the photoreduced Hb both in the N_2 and aerobic atmospheres showed identical bands with the normal oxyHb and meHb (Figure 4A). Even though the Mw of Hb is 64.5 kDa, it showed a higher relative Mw than albumin (67 kDa) as one of the markers in the Native-PAGE in the absence of sodium dodecyl sulfate, SDS, because the surface charge of the protein directly affect on the traveling distance during the electrophoresis. IEF of the photoreduced Hbs showed the presence of HbO_2 at pI = 7.0 as a dense band and a weak band at pI = 7.2 of a partially reduced Hb (Figure 4B). There was no band at 7.4 that corresponds to metHb.

The oxygen dissociation curve of the photoreduced Hb was identical with that of the normal HbO_2 (Data not shown here). The P_{50} and Hill number of the photoreduced Hb were 10.5 Torr and 1.8, respectively, and they were almost identical with the normal HbO_2 (11 Torr and 1.7, respectively).

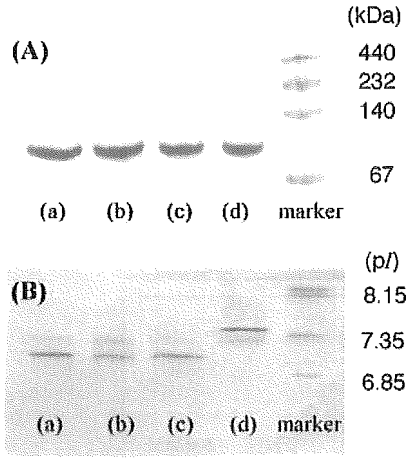

Figure 4. Native-PAGE (A) and IEF (B) of the photoreduced Hb in the presence of EDTA and FMN both in N_2 and aerobic atmospheres: (a) photoreduced Hb in N_2, (b) photoreduced Hb in air, (c) oxyHb, (d) metHb. In A, there was no change in the molecular weight of the Hb subunits. Since Native-PAGE does not include sodium dodecyl sulfate, the surface property of the protein directly affect on the traveling distance during electrophoresis. Therefore, Mw of Hb (Mw = 64.5 kDa) seemed much larger than albumin marker (Mw = 67 kDa). In B, the band at 7.4, which corresponded to metHb, almost disappeared in lanes a and b. No other bands were observed.

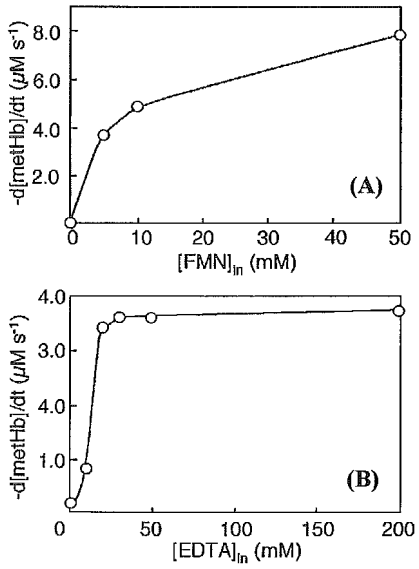

Figure 5. Influence of the concentrations of FMN and EDTA inside HbV on the initial rate of metHb reduction. (A) Influence of $[FMN]_{in}$ at the constant $[EDTA]_{in}$ = 20 mM. (B) Influence of $[EDTA]_{in}$ at the constant $[FMN]_{in}$ = 5 mM. [heme] = 10 μM in the cuvette, $[heme]_{in}$ = 21.7 mM. When $[EDTA]_{in}$ was higher than $[heme]_{in}$, the initial rate of metHb reduction was plateau.

Reduction of metHb in Hb-Vesicles. At first a diluted metHbV suspension ([heme] = 10 μM in a cuvette; $[heme]_{in}$ = 21.7 mM) was tested for photoreduction to analyze the kinetics. The initial rate of metHb reduction increased with increasing $[FMN]_{in}$ at a constant $[EDTA]_{in}$ (20 mM); however, the initial rate at $[FMN]_{in}$ = 10 mM was lower than twice that at $[FMN]_{in}$ = 5 mM (Figure 5A). At a constant $[FMN]_{in}$ (5 mM), increasing the $[EDTA]_{in}$ significantly facilitated the metHb photoreduction, however, the photoreduction rate did not increase above 20 mM (Figure 5B). This critical concentration is almost identical to $[heme]_{in}$ (21.7 mM). From these results, the rate-determining step of this system should be the electron transfer from an electron donor to the photoexcited FMN.

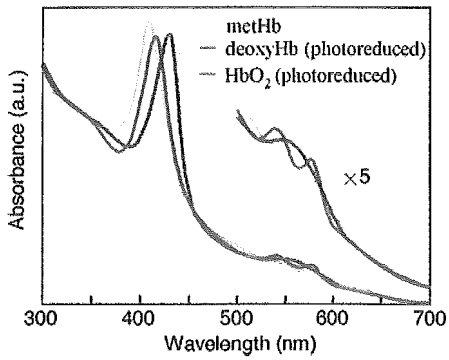

Figure 6. UV–visible spectra of HbV before irradiation (metHb), after photoreduction (deoxyHb), and its oxygenated form (HbO_2). $[EDTA]_{in}$ = 50 mM, $[FMN]_{in}$ = 5 mM, $[heme]_{in}$ = 21.7 mM. These spectra indicate the successful restoration of O_2-binding property of HbV.

The absorption spectra of the metHbV and the photoreduced HbV (λ_{max} = 430 nm) are shown in Figure 6. Due to the light scattering effect of the HbV particles, the turbidity was higher at a lower wavelength (*39*). Bubbling with an O_2 gas in a photoreduced HbV solution reversibly converted deoxyHb to HbO_2 with a characteristic shift of λ_{max} from 430 to 415 nm, indicating that the oxygen binding ability was successfully restored.

The concentration of [heme] in an HbV suspension for the intravenous infusion should be estimated to about 3–6 mM, which is significantly higher in comparison with 10 μM in a cuvette for the absorption spectral analysis. To test the photoreduction at a practical Hb concentration, a metHbV suspension ([heme] = 5.0 mM) was sandwiched between two glass plates and irradiated with visible light. The photoreduction proceeded quite promptly (Figure 7). Due to the thin liquid layer (ca. 10 μm in thickness), the effect of light scattering seen in Figure 6 is minimized. At the constant $[FMN]_{in}$ (5 mM) condition, the $[EDTA]_{in}$ of 10 and 20 mM were not enough to complete the reduction. At $[EDTA]_{in}$ = 50 mM, the photoreduction was significantly fast and the reaction was completed within 20 s with the characteristic λ_{max} of deoxyHb (430 nm). At $[FMN]_{in}$ = 100 mM and $[EDTA]_{in}$ = 20 mM, the initial reduction rate was the fastest; however, the reduction was not completed which was evident from the fact that the absorption at 430 nm in the Soret band was not high enough. The value of $[EDTA]_{in}$ should at least be higher than $[heme]_{in}$ (21.7 mM).

Quantum Yield of the Photoreduction Reactions. Table 2 summarizes the quantum yield, Φ, of various photoreduction conditions. The combination of metHb/FMN/EDTA showed the highest value (0.17) in an Ar atmosphere at [heme] = 0.1 mM. This was about 28 times higher than that for the photoreduction by the direct excitation of the N-band irradiating by near UV light (365 nm, Φ = 0.003–0.006) (*7*), and 4 times higher than the condition without an electron donor (0.04). In the case of HbV that coencapsulates FMN and EDTA, the concentrations of the components in the cuvette were much smaller, however, the concentrations in the nanoparticles (HbV) are much higher and the Φ for HbV was also very high (0.09–0.11). Probably due to the light scattering effect of HbV, Φ for HbV is slightly lower than that for the homogeneous Hb solution, but significantly higher than that for the N-band excitation (0.003–0.006).

Measurement of H_2O_2 in the metHb Photoreduction. Visible light irradiation to metHb([heme] = 20 μM)/FMN(5 μM)/EDTA(50 μM) under aerobic conditions

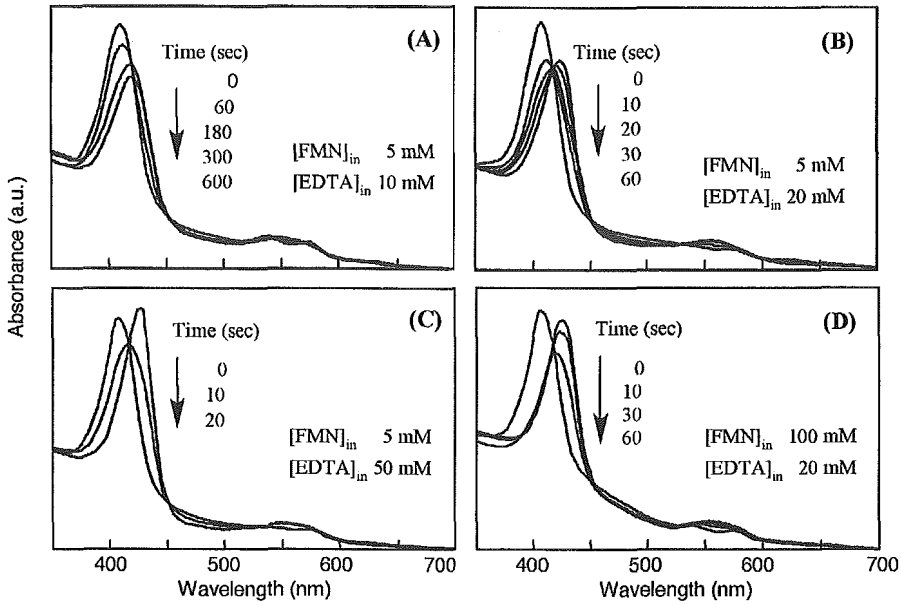

Figure 7. UV–visible spectral changes of HbV in a liquid layer sandwiched between two glass plates during photoreduction under aerobic conditions. The thickness of the layer was approximately 10 μm. Condition (C) ($[FMN]_{in}$ = 5 mM, $[EDTA]_{in}$ = 50 mM) showed the fastest rate of photoreduction, and the reaction was completed within 20 s. The arrows indicate the decrease in absorbance at 405 nm of MetHb with irradiation time.

Table 2. Quantum Yield (Φ) of Photoreduction of metHb and metHbV

	heme (mM)	FMN (mM)	electron donor (mM)	condition	λ_{ex} (nm)	Φ
metHb	0.1	0.01	EDTA (20)	in Ar	435	0.17
	0.1	0.01	Met (20)	in Ar	435	0.11
	0.1	0.01	no addition	in Ar	435	0.04
metHbV	0.01 (21.7)[a]	2.3×10^{-3} (5)[a]	EDTA (9.2×10^{-3}) (20)[a]	in Ar	435	0.09
	0.01 (21.7)[a]	46×10^{-3} (100)[a]	EDTA (9.2×10^{-3}) (20)[a]	in Ar	435	0.11
metHb	0.01	–	Trp (1.0)	in Ar	365	0.006[b]
	0.01	–	mannitol (100)	in CO	365	0.006[b]
	0.01	–	no addition	in CO	365	0.003[b]

[a] Concentrations of the components inside HbV; $[heme]_{in}$, $[FMN]_{in}$, $[EDTA]_{in}$. [b] Data from ref 7.

produced H_2O_2, and the fluorescent intensity of DBDA (λ_{em} = 404 nm) significantly increased (Figure 8a). The amount of H_2O_2 reached 40 μM at 120 s (Figure 8b). Irradiation to FMN alone produced 100 μM H_2O_2 for 120 s without any formation of $FMNH_2$. We confirmed that the irradiation to metHb alone did not produce H_2O_2 (data not shown here). The level of metHb photoreduction was less than 20% at 120 s (Figure 8c). A significant suppression of H_2O_2 generation was confirmed for the irradiation to metHbV and the H_2O_2 generation decreased to less than 20 μM, and the level of metHb photoreduction reached 50% at 120 s. A further increase in the level of photoreduction to 80% was confirmed when the partial oxygen pressure in the cuvette was regulated to 40 Torr; however, the amount of H_2O_2 could not be significantly reduced.

DISCUSSION

We found for the first time that the coencapsulation of concentrated Hb solution and the FMN/EDTA system in phospholipid vesicles (HbV) significantly facilitated the reduction of metHb by visible light irradiation (435 nm). This was evident from the Φ of the reaction, i.e., 0.17 for the Hb solution and 0.10 for the HbV suspension. The lowered Φ for HbV in comparison with that for a Hb solution is probably due to the light scattering of the illuminated visible light due to the particle of HbV (diameter, 250 nm) (*39*). However, they are much higher than that for the metHb photoreduction via direct photoexcitation of the N-band of the porphyrin ring in the UVA region (Φ = 0.006) (*7*). Even though the concentrations of the components in the cuvette were much lower for HbV than for the homogeneous Hb solution as shown in Table 2, the concentrations inside HbV were significantly higher and this condition facilitated the desired reactions (photoreduction of FMN and metHb) and suppressed the unwanted side reactions (generation of active oxygen species).

The reaction mechanism is that the photoexcited triplet FMN* rapidly receives an electron from the donor molecule, EDTA, to transform to the semiquinone followed by disproportionation to the two electron reduced form, $FMNH_2$. They are effective reducing agent to offer an electron to metHb. According to Yubisui et al., $FMNH_2$ reduces metHb with the rate constant of 5.5×10^6 M^{-1} s^{-1} (*22*), which is significantly faster than do glutathione (rate constant = 2.5×10^{-3} M^{-1} s^{-1}) (*27*) and ascorbic acid (3.0×10^{-3} M^{-1} s^{-1}) (*22*). The transient spectrum of the reduction of metHb by the photoreduced form of FMN demonstrated the completion of the reaction at 30 ns. Our result may be plausible because it is reported that a flavocytochrome showed complete photoreduction within 100 ns (*14*), measured by a laser flash-induced transient absorption difference spectra. The externally added FMN should more freely access to the protoporphyrin IX (heme) in the Hb molecule and would show a faster electron transfer. It is reported that the direct chemical conjugation of flavin to the propionic acid residue of heme significantly facilitates the electron transfer from flavin to heme in a reconstituted myoglobin (*40, 41*). Therefore,

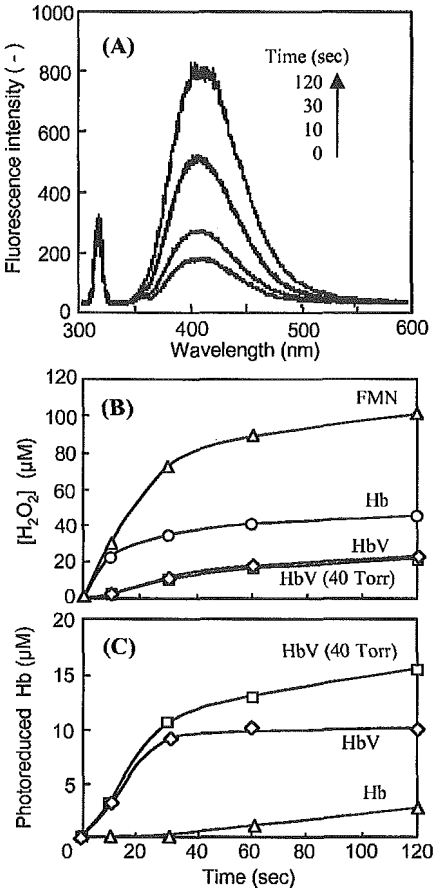

Figure 8. Detection of H_2O_2 using the fluorescence of DBDA during the photoreduction of Hb and HbV in the presence of FMN and EDTA. (A) An example of the fluorescence spectroscopy of the DBDA. The fluorescence intensity (λ_{em} = 404 nm) increased with time during the photoreduction of metHb solution under aerobic conditions (pO_2= 150 Torr). (B) Time course of the generation of H_2O_2 during the photoreduction of Hb and HbV under aerobic conditions (pO_2= 150 Torr), and HbV at pO_2 = 40 Torr. Irradiation to FMN alone was also tested as a reference (top curve) that produced 100 μM H_2O_2 for 120 s. Liberation of H_2O_2 from HbV was significantly suppressed in comparison with Hb solution. (C) The levels of metHb photoreduction during the measurement of H_2O_2 generation. The concentrations of heme (20 μM), FMN (5 μM), and EDTA (50 μM) in the cuvette were identical between the metHb solution and HbV suspension. For HbV, $[heme]_{in}$ = 21.6 mM, $[FMN]in$ = 5 mM, and $[EDTA]_{in}$ = 50 mM.

two propionic acid groups of a heme that directly face the outer aqueous phase of an Hb molecule should contribute to the electron transfer from the externally added FMN to the heme.

The side reaction of $FMNH_2$ is the reaction with O_2 to generate singlet O_2 ($^1O_2$) or H_2O_2 (*11*, *42*), due to the low redox potential of reduced flavin (E_m = −209 mV). However, according to the quantitative measurement of H_2O_2, photoreduction of metHbV significantly reduced the side reaction in comparison with the metHb solution. This effect is due to the highly concentrated condition inside metHbV: the photoexcited FMN* readily reacts with EDTA to generate $FMNH_2$, and it also readily reacts with concentrated metHb inside the HbV nanoparticle. However, for the complete removal of H_2O_2, further coencapsulation of catalase would be effective (*29*) in the presence of O_2. Of course, in the absence of O_2, only the metHb reduction proceeds.

We tried to find other optimal electron donors instead of EDTA, because it has been reported that the oxidized and decomposed EDTA elements contain acetaldehyde that might react with the lysine residues on a protein molecule (*10*), and EDTA is a strong chelator of Ca^{2+} as an anticoagulant and may require caution when using a large dosage. We confirmed that Met was effective secondary to EDTA, as reported by other researchers (*9*, *32*). Arg was also effective, but it was not stable against oxidation during incubation under aerobic conditions at 37 °C for 3 days. Met was stable against oxidation. However, the small amino acid, Met (Mw = 149), gradually leaks out from the HbV across the phospholipid bilayer membrane (data not shown). To minimize the leakage of an electron donor, larger molecules, Met-Met and Met-Glu, were tested. Unexpectedly, they did not show any contribution as an electron donor and retarded the reduction of FMN. The ribityl phosphate group in the FMN molecule can be an electron donor, because the photoreduction of FMN proceeds without the addition of an electron donor. The retardation by the peptides should be probably due to some interaction of these peptides with the ribityl phosphate group that may hinder the electron transfer to the isoalloxazine ring. Other amino acids such as Phe and Lys, and saccharides such as mannitol or maltotoriose, are effective as an electron donor; however, their reduction rates of FMN were much lower in comparison with EDTA. Interestingly, methanol and gaseous H_2 also showed facilitation. DTPA, a structure similar to EDTA, showed an effectiveness comparable with EDTA. EDTA is a well-known electron donor, and its larger size (Mw = 292) and four negative charges prevent leakage from the vesicles. We could not find a more effective electron donor in our study, but confirmed that IEF and native-PAGE did not demonstrate any change in the chemical modification of the photoreduced Hb in the presence of EDTA/FMN, and the O_2 binding property was successfully restored. Therefore, we tested coencapsulation of FMN/EDTA in HbV for the other studies.

When HbV is intravenously infused for the substitution of blood, the concentrations of Hb and the heme of HbV in plasma should reach 5 g/dL and 3.1 mM, respectively, or higher (*43*). These are much higher than the experimental conditions in Figures 1−4, and it is impossible to test such a highly concentrated solution in a cuvette because of the strong light scattering by the particles and absorption by Hbs. We thus tested sandwiching the solution with two glass plates, thus making a thin liquid layer between the glass plates. The thickness of the liquid membrane is approximately 10 μm, about twice the capillary diameter in in vivo peripheral tissues. Irradiation of visible light onto the liquid membrane of HbV coencapsulating FMN and EDTA showed significantly fast rates for the metHb photoreduction. Especially, the coencapsulation of FMN (5 mM) and EDTA (50 mM) completed the metHb photoreduction within only 20 s. This significantly fast photoreduction system would be applicable to the transcutaneous irradiation of visible light to the body for the rejuvenation of HbV when the metHb content increased after the infusion of HbV.

In our study we established an efficient photoreduction system in a nanoparticle as shown in Figure 9. The illuminated visible light excites FMN to convert it to FMN*, and this reacts with an electron donor and transforms to $FMNH_2$, that subsequently reduces ferric metHb to its ferrous form. The reduced Hb can then reversibly bind O_2. Irrespective of the blood substitutes, one advantage of coencapsulation in a nanoparticle is that the concentrations of the components in the vesicles (nanoenvironment) are very high. Accordingly, the desired reactions are significantly accelerated and the

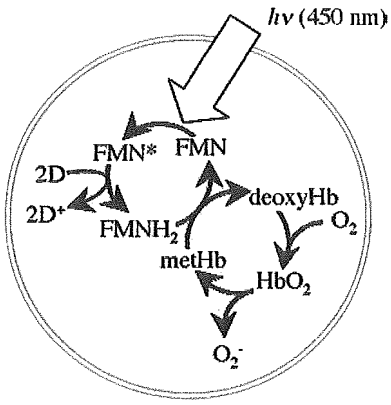

Figure 9. MetHb photoreduction system in a nanoparticle (HbV) using FMN and an electron donor (D), and recovery of the O_2-binding property.

unwanted side reaction is minimized in comparison with the homogeneous solution. To completely eliminate the side reaction of $FMNH_2$ and O_2, photoreduction under anaerobic conditions or coencapsulation of a radical scavenger, such as catalase, would be effective (*29*, *30*). RBC contains NADPH-flavin reductase to reduce metHb (*21*), and the reduced form of flavin is susceptible to react with O_2 as a side reaction. However, our results imply that the highly concentrated condition in RBCs and well-organized radical scavenging system should contribute to the effective metHb reduction in RBCs.

ACKNOWLEDGMENT

Supported by Health Sciences Research Grants (Research on Pharmaceutical and Medical Safety, Artificial Blood Project), the Ministry of Health and Welfare, Japan, 21 COE "Practical Nano-Chemistry" from MEXT, Japan, and Grants in Aid for Scientific Research from the Japan Society for the Promotion of Science (B16300162).

LITERATURE CITED

(1) Tracewell, C. A., Cua, A., Stewart, D. H., Bocian, D. F., and Brudvig, G. W. (2001) Characterization of carotenoid and chlorophyll photooxidation in photosystem II. *Biochemistry 40*, 193−203.

(2) Vorkink, W. P., and Cusanovivh, M. A. (1974) Photoreduction of horse heart cytochrome *c*. *Photochem. Photobiol. 19*, 205−215.

(3) Adar, F., and Yonetani, T. (1978) Resonance Raman spectra of cytochrome oxidase. Evidence for photoreduction by laser photons in resonance with the Soret band. *Biochim. Biophys. Acta 502*, 80−86.

(4) Kitagawa, T., and Nagai, K. (1979) Quaternary structure-induced photoreduction of haem of haemoglobin. *Nature 281*, 503−504.

(5) Kitagawa, T., Chihara, S., Fushitani, K., and Morimoto, H. (1984) Resonance Raman study of subunit assembly dependent photoreduction of heme of extracellular giant hemoglobin. *J. Am. Chem. Soc. 106*, 1860−1862.

(6) Pierre, J., Bazin, M., Debey, P., and Santus, P. (1982) One-electron photoreduction of bacterial cytochrome P-450 by ultraviolet light. *Eur. J. Biochem. 124*, 533−537.

(7) Sakai, H., Onuma, H., Umeyama, M., Takeoka, S., and Tsuchida E. (2000) Photoreduction of methemoglobin by irradiation in the near-ultraviolet region. *Biochemistry 39*, 14595−14602.

(8) McCormick, D. B., Koster, J. F., and Veeger, C. (1967) On the mechanism of photochemical reductions of FAD and FAD-dependent flavoproteins. *Eur. J. Biochem. 2*, 387−391.

(9) Heelis, P. F., Parsons, B. J., Phillips, G. O., and McKellar, J. F. (1979) The photoreduction of flavins by amino acids and EDTA. A continuous and flash photolysis study. *Photochem. Photobiol. 30*, 343−347.

(10) Traber, R., Kramer, H. E. A., and Hemmerich, P. (1982) Mechanism of light-induced reduction of biological redox centers by amino acids. A flash photolysis study of flavin photoreduction by ethylenediaminetetraacetate and nitrilotriacetate. *Biochemistry 21*, 1687−1693.

(11) Massey, V., Strickland, S., Mayhew, S. G., Howell, L. G., Engel, P. C., Matthews, R. G., Schuman, M., and Sullivan, P. A. (1969) The production of superoxide anion radicals in the reaction of reduced flavins and flavoproteins with molecular oxygen. *Biochem. Biophys. Res. Commun.* 36, 891−897.

(12) Massey, V., Stankovich, M., and Hemmerich, P. (1978) Light-mediaated reduction of flavoproteins with flavins as catalyst. *Biochemistry 17*, 1−8.

(13) Cusanovich, M. A., Meyer, T. E., and Tollin, G. (1985) Flavocytochrome *c*. Transient kinetics of photoreduction by flavin analogues. *Biochemistry 24*, 1281−1287.

(14) Sharp, R. E., Moser, C. C., Rabanal, F., and Dutton, P. L. (1998) Design, synthesis, and characterization of a photoactivatable flavocytochrome molecular maquette. *Proc. Natl. Acad. Sci. U.S.A.* 95, 10465−10470.

(15) Hazzard, J. T., Govindaraj, S., Poulos, T. L., and Tollin, G. (1997) Electron transfer between the FMN and heme domains of cytochrome P450 μ_B-3. *J. Biol. Chem. 272*, 7922−7926.

(16) Shumyantseva, V. V., Bulko, T. V., Schmid, R. D., and Archakov, A. I. (2002) Photochemical properties of a riboflavins/cytochrome P450 2B4 comples. *Biosensors Bioelecronics 17*, 233−238.

(17) Shumyantseva, V. V., Bulko, T. V., Schmid, R. D., and Archakov, A. I. (2000) Flavocytochrome P450 2B4 photoreduction. *Biophysics 45*, 982−987 (Translated from *Biofizika*).

(18) Masuda, S., and Bauer, C. E. (2002) AppA is a blue light photoreceptor that antirepresses photosynthesis gene expression in Rhodobacter sphaeroides. *Cell 110*, 613−623.

(19) Tsubota, K., Laing, R. A., and Kenyon, K. R. (1987) Noninvasive measurements of pyridine nucleotide and flavoprotein in the lens. *Invest. Ophthalmol. Vis. Sci. 28*, 785−789.

(20) Brown, W. D., and Synder, H. E. (1969) Nonenzymatic reduction and oxidation of myoglobin and hemoglobin by nicotinamide adenine dinucleotides and flavins. *J. Biol. Chem. 244*, 6702−6706.

(21) Yubisui, T., Takeshita, M., and Yoneyama, Y. (1980a) Reduction of methemoglobin through flavin at the physiological concetration by NADPH-flavin reductase of human erythrocytes. *J. Biochem. 87*, 1715−1720.

(22) Yubisui, T., Matsukawa, S., and Yoneyama, Y. (1980b) Stopped flow studies on the nonenzymatic reduction of methemoglobin by reduced flavin mononucleotide. *J. Biol. Chem. 255*, 11694−11697.

(23) Tsuchida, E. (1998) *Blood Substitutes: present and future perspectives* (Tsuchida, E., Ed.) Elsevier Science, New York.

(24) Takeoka, S., Ohgushi, T., Ohmori, T., Terase, T., and Tsuchida, E. (1996) Layer controlled hemoglobin vesicles by interaction of hemoglobin with phospholipid assembly. *Langmuir 12*, 1775−1779.

(25) Sakai, H., Takeoka, S., Park, S. I., Kose, T., Nishide, H., Izumi, Y., Yoshizu, A., Kobayashi, K., and Tsuchida, E. (1997) Surface modification of hemoglobin vesicles with poly(ethyleneglycol) and effects on aggregation, viscosity, and blood flow during 90% exchange transfusion in anesthetized rats. *Bioconjugate Chem. 8*, 23−30.

(26) Szebeni, J., Hauser, H., Eskelson, C. D., Watson, R. R., and Winterhalter, K. H. (1988) Interaction of hemoglobin derivatives with liposomes. Membrane cholesterol protects against the changes of hemoglobin. *Biochemistry 27*, 6425−6434,

(27) Takeoka, S., Sakai, H., Kose, T., Mano, Y., Seino, Y., Nishide, H., and Tsuchida, E. (1997) Methemoglobin formation in hemoglobin vesicles and reduction by encapsulated thiols. *Bioconjugate Chem. 8*, 539−544.

(28) Sakai, H., Tomiyama, K., Sou, K., Takeoka, S., and Tsuchida, E. (2000) Poly(ethyleneglycol)-conjugation and

deoxygenation enable long-term preservation of hemoglobin vesicles as oxygen carriers. *Bioconjugate Chem. 11*, 425–432
(29) Teramura, Y., Kanazawa, H., Sakai, H., Takeoka, S., and Tsuchida, E. (2003) The prolonged oxygen -carrying ability of Hb vesicles by coencapsulation of catalase in vivo. *Bioconjugate Chem. 14*, 1171–1176.
(30) D'Agnillo, F., and Chang, T. M. (1998) Polyhemoglobin-superoxide dismutase-catalase as a blood substitute with antioxidant properties. *Nat. Biotechnol. 16*, 667–71.
(31) Chang, T. M., Powanda, D., and Yu WP. (2003) Analysis of polyethylene-glycol-polylactide nano-dimension artificial red blood cells in maintaining systemic hemoglobin levels and prevention of methemoglobin formation. *Artif. Cells Blood Substitutes Immobilization Biotechnol. 31*, 231–47.
(32) Everse, J. (1994) Photochemical reduction of methemoglobin and methemoglobin derivatives. *Methods Enzymol. 231*, 524–536.
(33) Sakai, H., Takeoka, S., Yokohama, H., Seino, Y., Nishide, H., and Tsuchida, E. (1993) Purufication of concentrated Hb using organic solvent and heat treatment. *Protein Expression Purif. 4*, 563–569.
(34) Sakai, H., Yuasa, M., Onuma, H., Takeoka, S., and Tsuchida, E. (2000) Synthesis and physicochemical characterization of a series of hemoglobin-based oxygen carriers: objective comparison between cellular and acellular types. *Bioconjugate Chem. 11*, 56–64.
(35) Hatchard, C. G., and Parker, C. A. (1956) A new sensitive chemical actinometer II. Potasium ferrioxalate as a standard chemical actinometer. *Proc. R. Soc. London 235*, 518–536.
(36) Wegner, E. E., and Adamson, A. W. (1966) Photochemistry of complex ions. III. Absolute quantum yields for the photolysis of some aqueous chromium (III) complexes. Chemical actinometry in the long wavelength visible region. *J. Am. Chem. Soc. 88*, 394–404.
(37) Sou, K., Naito, Y., Endo, T., Takeoka, S., and Tsuchida, E. (2003) Effective encapsulation of proteins into size-controlled phospholipid vesicles using freeze–thawing and extrusion. *Biotechnol. Prog. 19*, 1547–1552.
(38) Sou, K., Endo, T., Takeoka, S., and Tsuchida, E. (2000) Poly(ethylene glycol)-modification of the phospholipid vesicles by using the spontaneous incorporation of poly(ethylene glycol)-lipid into the vesicles. *Bioconjugage Chem. 11*, 372–379.
(39) Sakai, H., Tomiyama, K., Masada, Y., Takeoka, S., Horinouchi, H., Kobayashi, K., and Tsuchida, E. (2003) Pretreatment of serum containing Hb-vesicels (oxygen carriers) to avoid interference in clinical laboratory tests. *Clin. Chem. Lab. Med. 41*, 222–231.
(40) Hamachi, I., Nomoto, K., Tanaka, S., Tajiri, Y., and Shinkai, S. (1994) Self-sufficient electron injection from NADH to the active center of flavin-pendant myoglobin. *Chem. Lett. 1994*, 1139–1142.
(41) Matsuo, T., Hayashi, T., and Hisaeda, Y. (2002) Reductive activation of dioxygen by a myoglobin reconstituted with a flavohemin. *J. Am. Chem. Soc. 124*, 11234–11235.
(42) Frati, E., Khatib, A., Front, P., Panasyuk, A., Aprile, F., and Mitrovic, D. R. (1997) Degradation of hyaluronic acid by photosensitized riboflavin in vitro. Modulation of the effect by transition metals, radical quenchers, and metal chelators. *Free Rad. Biol. Med. 22*, 1139–1144.
(43) Sakai, H., Horinouchi, H., Masada, Y., Yamamoto, M., Takeoka, S., Kobayashi, K., Tsuchida, E. (2004) Hemoglobin-vesicles suspended in recombinant human serum albumin for resuscitation from hemorrhagic shock in anesthetized rats. *Crit. Care Med. 32*, 539–545.

BC049913Z

Hemorrhagic Shock Resuscitation With an Artificial Oxygen Carrier, Hemoglobin Vesicle, Maintains Intestinal Perfusion and Suppresses the Increase in Plasma Tumor Necrosis Factor-α

Akira Yoshizu,* Yotaro Izumi,* Sungick Park,‡ Hiromi Sakai,‡ Shinji Takeoka,‡ Hirohisa Horinouchi,* Eiji Ikeda,† Eishun Tsuchida,‡ and Koichi Kobayashi*

It is known that damage to the intestinal mucosa followed by systemic inflammatory response is one of the leading causes of shock related morbidity and mortality. In this study, we examined the ability of an artificial oxygen carrier hemoglobin vesicle (HbV) to sustain systemic and intestinal perfusion during hemorrhagic shock. In rabbits, hemorrhagic shock (40% of the estimated blood volume) was resuscitated with 5% albumin (alb group), HbV suspended in 5% albumin (HbValb group), or washed red blood cells suspended in 5% albumin (RBCalb group). Plasma tumor necrosis factor (TNF)-α level was measured in rats under the same experimental protocol. No significant intergroup differences were seen in systemic hemodynamics. In contrast, parameters of intestinal perfusion significantly deteriorated in the alb group but were equally well sustained in the HbValb and RBCalb groups. Also, a significant increase in plasma TNF-α level was seen in the alb group but not in the RBCalb or HbValb groups. These results indicate the proficient oxygen transporting capability of HbV and its potential efficacy in shock resuscitation. *ASAIO Journal* 2004; 50:458–463.

Blood replacement is the basic therapeutic modality when a considerable amount of blood is lost because of trauma or major surgery. Despite the recent progress in transfusion medicine, enormous investments are still necessary to establish and sustain the systems from blood donation to transfusion. Donated blood inspections to avoid the side effects of homologous blood transfusion, such as transfusion associated infectious disease, alloimmunization, and graft *versus* host diseases are still essential.[1,2] To overcome these problems associated with transfusion, development of artificial blood substitutes is important. To this end, we have developed several types of artificial oxygen carriers and have evaluated the efficacy of these compounds in various animal models.[1] Among these compounds, hemoglobin vesicle (HbV), a form of liposome encapsulated hemoglobin, is rapidly approaching clinical trials. The cellular structure of HbV, similar to red blood cells, shields all of the physiologic effects of acellular Hb solutions.[3–5] We have studied the oxygen transporting capabilities of HbV, using several exchange transfusion and hemorrhagic shock models.[6–10] In these studies, we have shown that HbV effectively restores the systemic circulation in hemorrhagic shock.

It is known that gastrointestinal perfusion is compromised at a relatively early stage in hypovolemic shock to sustain the systemic circulation to other vital organs.[11] This, however, causes damage to the intestinal mucosa followed by systemic inflammatory response syndrome (SIRS) or sepsis, which is one of the leading causes of shock related morbidity and mortality.[12,13] In the present study, we examine the ability of HbV to sustain not only systemic but also intestinal perfusion to further evaluate the efficacy of HbV in hemorrhagic shock.

Materials and Methods

Animal Care

The experimental protocol was fully approved by the Laboratory Animal Care and Use Committee of Keio University, School of Medicine. It also complies with Guidelines for the Care and Use of Laboratory Animals of Keio University, School of Medicine. All rabbits and rats were housed in groups of two in standard cages and were provided with food and water in a temperature controlled room on a 12 hour dark/light cycle.

Preparation of Hemoglobin Vesicle Suspended in 5% Albumin

HbV suspension was prepared in a similar manner as previously reported in the literature.[14,15] In brief, a purified and concentrated human hemoglobin solution (40 g/dl) was obtained from outdated red blood cells.[16] Added to this purified hemoglobin solution were pyridoxal 5'-phosphate (18 mM, Merck Co., Frankfurter, Germany) as an allosteric effector and homocysteine (Aldrich Co., Milwaukee, WI) as a reductant of methemoglobin. The lipid bilayer of HbV was composed of Presome PPG-I (Nippon Fine Chem. Co., Osaka, Japan) containing 1,2-dipalmitoyl-*sn*-glycero-3-phosphatidylcholine, (DPPC), cholesterol, and 1,2-dipalmitoyl-*sn*-glycero-3-phos-

From the *Department of Surgery and the †Department of Pathology, Keio University School of Medicine, Tokyo, Japan; and the ‡Advanced Research Institute for Science and Engineering, Waseda University, Tokyo, Japan.

Submitted for consideration November 2003; accepted for publication in revised form June 2004.

Correspondence: Koichi Kobayashi, Director and Chief, Division of Thoracic Surgery, Department of Surgery, Keio University School of Medicine, Tokyo 160–8582, Japan.

DOI: 10.1097/01.MAT.0000136508.51676.EF

Table 1. Physicochemical Properties of PEG Modified HbV Suspended in Human Serum Albumin

Hb (g/dl)	10
Lipid (g/dl)	6.2
Hb/lipid (g/g)	1.61
Diameter (nm)	251 ± 87
P_{50} (torr)	32
Hill number	2.2
Viscosity (cP at 358 s^{-1})	3.7
HbCO (%)	2
MetHb (%)	3

PEG,.

phatidylglycerol (DPPG), which were purchased from Nippon Fine Chem. Co. (Osaka, Japan), and α-tocopherol was added to these at the composition so that the molar ratios for DPPC: cholesterol:DPPG: α-tocopherol became 5:5:1:0.1. The surface of the HbV was modified with poly(ethylene glycol) (Mw: 5 kDa, 0.3 mol% of the lipids in the outer surface of vesicles) using 1,2-distearoyl-*sn*-glycero-3-phosphatidylethanolamine-*N*-poly(ethylene glycol) (Sunbright DSPE-50H, H-form, NOF Co., Tokyo, Japan). HbVs were suspended in 5% human serum albumin (alb) containing 160 mEq/L sodium and 107 mEq/L chloride (Albumin 5%-cutter, Bayer) and filtered through sterilizable filters (Dismic, Toyo Roshi Co., Tokyo, Japan, pore size: 0.45 micrometer). The whole procedure was performed at temperatures below 10°C in a sterile environment.

The properties of HbV suspended in alb (HbValb) are summarized in **Table 1**. The amount of oxygen release was calculated to be 6.2/100 ml. This is close to 7.0/100 ml of human blood (hemoglobin concentration 15 g/dl) because of, theoretically, the increased oxygen transporting efficiency (the difference in oxygen saturation between 40 and 110 mm Hg PO_2) of HbV compared with human red blood cells (37% to 28%, respectively).

Preparation of Washed Rabbit (Rat) Red Blood Cells Suspended in 5% Albumin

Blood samples were withdrawn from rabbits/rats into heparinized syringes and centrifuged to obtain a red blood cell concentrate. This was washed twice to remove plasma components and buffy coat by resuspension in 5% human serum albumin and centrifugation (4,300 rpm, 10 min). The hemoglobin concentration was adjusted to 10 g/dl, equivalent to that of HbValb.

Hemorrhagic Shock Resuscitation

Animal preparation was performed as follows (**Figure 1**). Male Japanese white rabbits (3.0 ± 0.4 kg) were anesthetized with intramuscular injection of ketamine hydrochloride (50 mg/kg) and intravenous injection of pentobarbital sodium (20 mg/kg) through the marginal ear vein. The body temperatures of the animals were maintained between 36 and 37°C by a heating lamp during the experiment.

Tracheostomy tubes were placed to secure the airway. The animals breathed spontaneously during the experiment. A polyethylene tube (outer diameter 1.7 mm, ATOM Japan) was introduced into the right carotid artery for blood withdrawal and connected to a pressure transducer (Polygraph System,

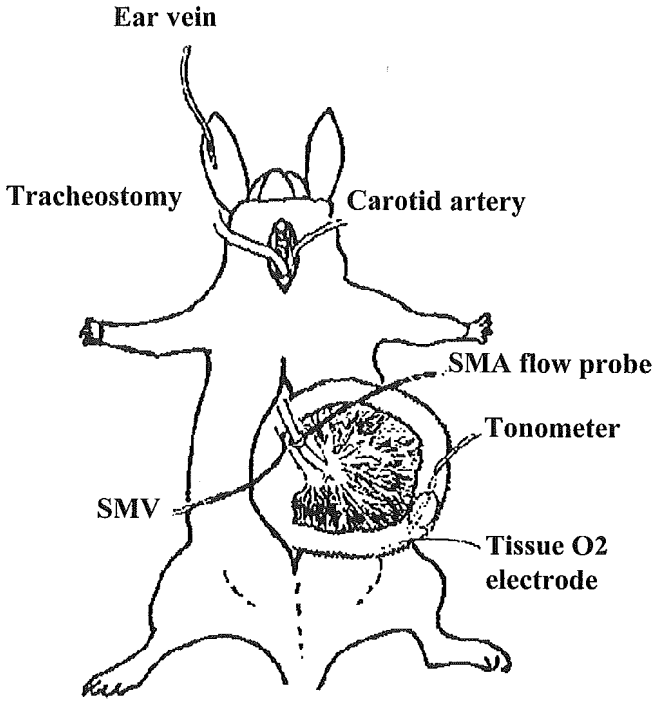

Figure 1. Schematic representation of the shock resuscitation experiment in the rabbit is shown. SMA, superior mesenteric artery; SMV, superior mesenteric vein.

Nihon Koden, Tokyo Japan) for continuous mean arterial pressure (MAP) monitoring. A median abdominal incision was made, and the superior mesenteric artery (SMA) was identified and dissected from surrounding tissue close to its origin from the aorta. A 2 mm ultrasonic flow probe (20 MHz, Crystal Biotech, Hopkinton, MA) was placed around the root of SMA and connected to a blood flow meter for measurement of SMA flow and heart rate. A small vein in the mesentery was ligated distally and cannulated with polyethylene catheter (PE-20). The catheter was advanced 5–10 cm proximally until the tip was located in the superior mesentric vein (SMV) for sampling of venous blood. For arterial and venous blood gas measurements, Corning 170 pH/blood gas analyzer (Corning Medical, Medfield, MA) was used. Hemoglobin concentration was determined by hemoglobin analyzer, Sysmex E-400 (Toa Medical Electronics Co, LTD, Kobe, Japan).

A sigmoid tonometor (Tonomiter Tonometorics) was positioned in the duodenum 2–3 cm from the pylorus for intestinal mucosal pH (pHi) measurements. The pHi was determined from partial carbon dioxide pressure (PCO_2) in the tonometer saline, the bicarbonate concentration, and the Henderson-Hasselbalch equation (I):

$$pHi = 6.1 + \log_{10}(HCO_3^-/(0.22 \cdot PCO_2 \cdot k)) \quad (1)$$

A needle type polarographic oxygen electrode (Intermedical, Tokyo, Japan) was inserted into the submucosa of the small intestine for continuous intestinal submucosal tissue oxygen tension measurements.

Approximately 20 minutes was allowed for MAP, SMA blood flow, and tissue oxygen tension measurements to stabilize. Hemorrhagic shock was induced by withdrawal of 40% of the estimated total blood volume of the rabbit from the right

carotid artery at a rate of 10 ml/min (3 ml/kg/min). Approximately 10 minutes after bleeding, they were infused with the lost volume *via* the marginal ear vein at the same rate with 5% albumin (alb group, n = 6), HbValb (HbValb group, n = 6), or washed rabbit red blood cell (RBCalb group, n = 6). This procedure was repeated twice. Arterial (carotid artery) and SMV blood samples were drawn before bleeding (BASAL), after first bleeding (BL1), after first infusion (IN1), after second bleeding (BL2), after second infusion (IN2), and at 30 min after the second infusion (AFTER30); pHi was measured at BASAL, BL2, IN2, and AFTER30.

Histologic Examination

After completion of the experiment, the animals were killed by pentobarbital overdose. The heart, lung, kidney, liver, spleen, and small intestine were removed and fixed in 10% formalin. The tissues were embedded in paraffin, and the sections were stained with hematoxylin and eosin for light microscopic examinations.

Tumor Necrosis Factor-α Measurements

Male Wistar rats (364 ± 15 g) were used for the experiment. They were anesthetized with intraperitoneal injections of pentobarbital (50 mg/kg). A longitudinal midline ventral cervical incision was made, and catheters (PE-20 tubing, outer diameter 0.8 mm, inner diameter 0.5 mm) were introduced into the right jugular vein for infusion and into the right common carotid artery for blood withdrawal. Shock resuscitation was performed following the protocol in the rabbit. Forty percent of the estimated total blood volume was drawn from the right carotid artery at a rate of 1 ml/min (3 ml/kg/min). After bleeding, they were infused *via* the jugular vein with the same rate and volume of 5% albumin (n = 6), HbValb (n = 6), or washed rat red blood cell (n = 6). This procedure was repeated twice. Thirty minutes after the second infusion, corresponding to AFTER30, blood was sampled from the carotid artery. After centrifuging the blood at 4,300 rpm for 10 minutes, the plasma component was separated and stored at −80°C until measurement. TNF-α was measured by enzyme linked immunosolvent assay (ELISA) using Genzyme-Technic rat TNF-α determination kit.

Data Analysis

Data are shown as mean ± SD, as percentage changes or differences from basal values. The error bars in the figures indicate SD. Data were compared between groups at corresponding time points by Mann-Whitney *U* test (StatView, Institute Inc., Cary, NC). The level of confidence was placed at 95% for all experiments.

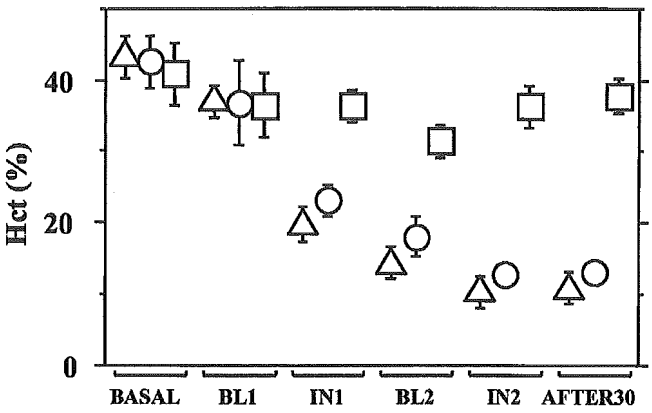

Figure 2. Changes in hematocrit in rabbits. Time points: before bleeding (BASAL), after first bleeding (BL1), after first infusion (IN1), after second bleeding (BL2), after second infusion (IN2), and at 30 min after the second infusion (AFTER30). Triangle, alb group; circle, HbValb group; square, RBCalb group.

Results

Hemorrhagic Shock Resuscitation

Hemodynamic, blood gas, and intestinal measurements were performed in rabbits. After IN2, the hematocrit (Hct) (**Figure 2**) decreased from approximately 40% to 10% in both alb and HbValb groups. This indicated that approximately 40% of the circulating blood volume was actually replaced twice.

In **Table 2**, values at BASAL are shown for parameters representing hemodynamics, arterial blood gas, and intestinal perfusion. No significant intergroup differences were observed regarding these parameters. Therefore, the subsequent data changes are shown as percentage changes or differences from values at BASAL.

Mean arterial pressure (MAP) (**Figure 3a**) declined sharply after bleeding but rapidly recovered after infusion. There were no significant differences between groups. Heart rate (HR) (**Figure 3b**) tended to decrease slightly during the course of the experiment, but there were no significant differences between groups. Superior mesenteric aortic (SMA) blood flow (**Figure 3c**) declined sharply after bleeding but rapidly recovered after

Table 2. Basal Values of Measured Parameters

Basal Values	Alb Group	HbValb Group	RBCalb Group
Mean arterial pressure (mm Hg)	120 ± 13	110 ± 21	132 ± 19
Heart rate (beats/min)	233 ± 23	250 ± 33	240 ± 45
PaO_2 (Torr)	97.1 ± 11.0	92.3 ± 7.8	99.0 ± 9.7
$PaCO_2$ (Torr)	31.0 ± 4.7	30.1 ± 2.9	30.4 ± 2.6
Arterial base excess (mmol/L)	−3.2 ± 3.6	−2.9 ± 4.2	−4.8 ± 2.0
Superior mesenteric arterial flow (ml/min/kg)	22.0 ± 10.0	32.2 ± 11.2	36.9 ± 21.1
Intestinal mucosal pH	7.4 ± 0.1	7.4 ± 0.3	7.4 ± 0.1
Intestinal tissue PO_2 (Torr)	21.4 ± 3.4	18.4 ± 4.8	19.8 ± 6.0
Superior mesenteric venous PO_2 (Torr)	45.8 ± 3.1	42.2 ± 9.4	51.4 ± 8.9

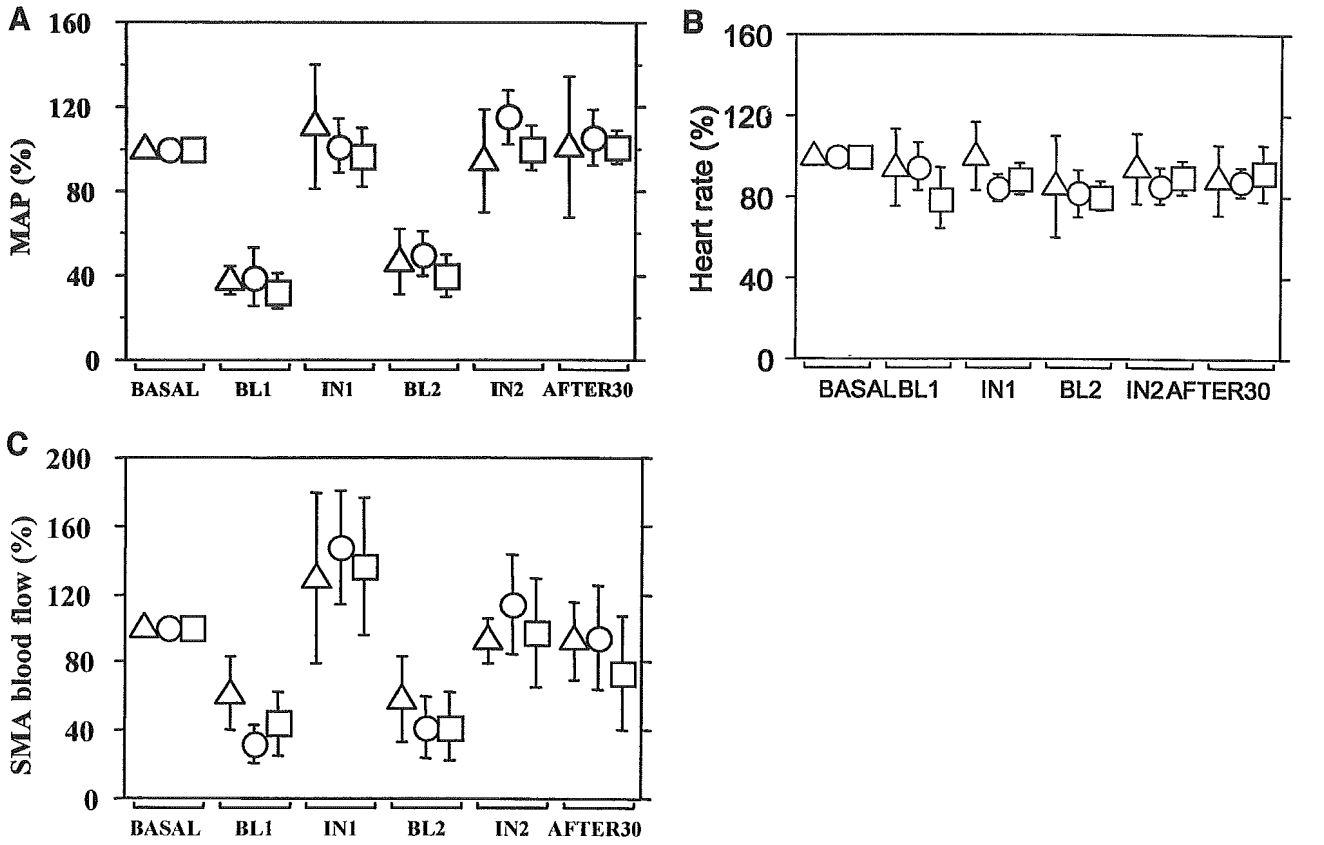

Figure 3. Changes in hemodynamic parameters from basal values in rabbits. Time points: before bleeding (BASAL), after first bleeding (BL1), after first infusion (IN1), after second bleeding (BL2), after second infusion (IN2), and at 30 min after the second infusion (AFTER30). Triangle, alb group; circle, HbValb group; square, RBCalb group.

infusion. There were no significant differences between groups.

Arterial oxygen tension (PaO_2) (**Figure 4a**) tended to increase slightly during bleeding and infusion in all the groups. There were no significant differences between groups. Arterial carbon dioxide tension ($PaCO_2$) (**Figure 4b**) remained stable throughout the study in all the groups. Systemic base excess (BE) (**Figure 4c**) declined significantly in the alb group compared with the RBCalb group at BL2. At IN2 and AFTER30, BE in the alb group was significantly lower compared with both HbValb and RBCalb groups.

In the alb group, pHi (**Figure 5a**) declined significantly compared with both HbValb and RBCalb groups beyond BL2. Intestinal tissue oxygen tension (**Figure 5b**) declined after bleeding but recovered to baseline by infusion in the HbValb and RBCalb groups but not in the alb group. The differences were significant beyond IN2. Superior mesenteric venous (SMV) oxygen tension (**Figure 5c**) declined sharply after bleeding but rapidly recovered close to baseline after infusion in all the groups. However, at AFTER30, it significantly increased in the alb group compared with both HbValb and RBCalb groups.

Histologic Examination

No significant abnormalities or differences among groups were observed in any of the organs examined in the rabbits.

Plasma Level of Tumor Necrosis Factor-α

In the rats, TNF-α concentration in plasma (pg/ml) was increased approximately 40-fold in the alb group (4,634 ± 4,276) compared with the HbValb group (124 ± 65). In the RBCalb group, it was below detection limit (<25).

Discussion

Peripheral tissue perfusion is controlled in response to changes in systemic hemodynamics. Intestinal perfusion is known to be one of the first to decline in hemorrhagic shock when the redistribution of systemic blood flow occurs to other vital organs such as the heart and the brain. However, it is also known that the loss of adequate intestinal function caused by insufficient perfusion leads to serious complications such as bacterial translocation and cytokine production,[17] which can eventually lead to mortality even when other vital organs are initially well sustained. It has been shown that indices such as intestinal mucosal pH are valid in assessing the severity of shock, as well as predicting prognosis.[18] To this end, in this study, we observed parameters of intestinal perfusion in addition to systemic hemodynamic parameters to evaluate the applicability of HbV in hemorrhagic shock resuscitation.

In the present study, in the rabbits, shock resuscitation with albumin satisfactorily restored parameters such as MAP and HR. Lung function was also maintained as shown by the

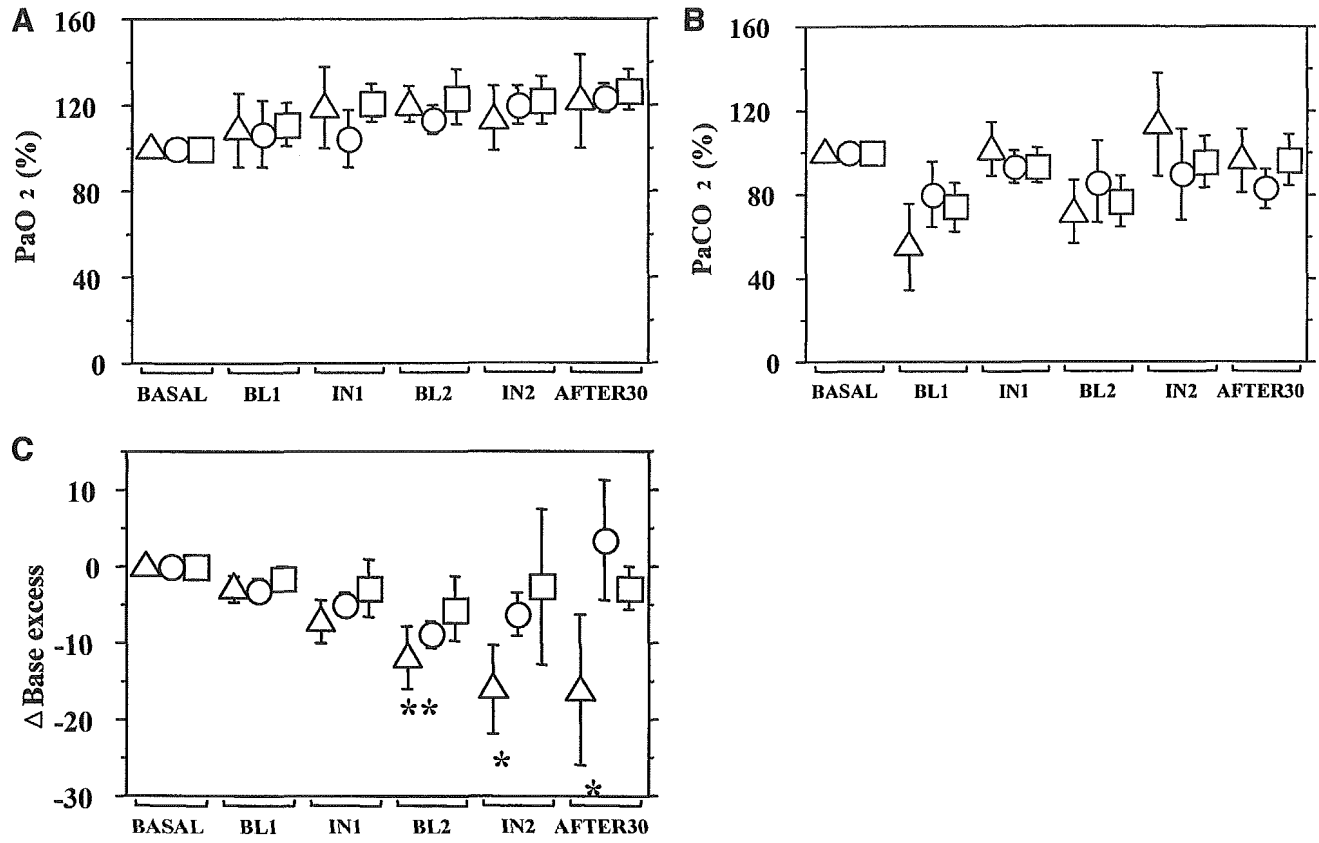

Figure 4. Changes in arterial blood gas parameters from basal values in rabbits. Time points: before bleeding (BASAL), after first bleeding (BL1), after first infusion (IN1), after second bleeding (BL2), after second infusion (IN2), and at 30 min after the second infusion (AFTER30). Triangle, alb group; circle, HbValb group; square, RBCalb group. *$p < 0.05$ *vs.* HbValb and RBCalb groups; **$p < 0.05$ *vs.* RBCalb group.

systemic oxygen and carbon dioxide tension. However, systemic base excess significantly declined in the alb group indicating peripheral hypoperfusion, and our data show that one such organ is the intestine. Even though SMA blood flow was maintained, lack of peripheral perfusion in the alb group was depicted by the significant decline in pHi and intestinal tissue oxygen tension. The subsequent significant increase in SMV oxygen tension was most likely brought about by the shutdown of peripheral circulation leading to shunting of SMA blood. We consider that all of these changes resulted from the impairment in cardiac function caused by decreased oxygen content in the alb group, which subsequently limited the oxygen delivery to the cardiac muscles. It is likely that a longer observation period was required for these changes to become morphologically apparent on histology. However, most of the animals in the alb group could not survive beyond 30 minutes after the second infusion in this study design.

TNF-α is believed to be an important mediator of SIRS. It has been reported that the intestine is a major source of TNF-α production during hemorrhagic shock.[19] We used rats for the measurement of plasma TNF-α. Ideally, the assay for TNF-α should have been performed in rabbits. However, we were not able to find an appropriate TNF-α antibody to perform ELISA in rabbits. On the other hand, we had previously performed TNF-α assay in the rat, and the assay technique was well established. In our preliminary shock resuscitation experiments in rats, we found that withdrawal of 40% of estimated circulating blood volume reduced MAP to approximately 40% of baseline (data not shown). Also, we have previously reported that withdrawal of 50% of estimated circulating blood volume in rats reduced MAP to approximately 20% of baseline, and base excess declined from 0 to approximately −6.[9] From these data, we extrapolated that the hemodynamic changes would be similar in rats compared with rabbits under the same shock resuscitation protocol. Therefore, we decided to perform the TNF-α measurements in rats. Under the same experimental protocol, we saw a significant increase in the plasma levels of TNF-α in the alb group. This was effectively suppressed in the HbValb group, although not quite to the level of RBCalb group. In this particular experiment, there is no evidence to show that the hemodynamic changes or the changes in the intestinal parameters were the same in the rats compared with the rabbits. However, we believe that the substantial intergroup differences in TNF-α in the rats, although not directly, provide support that intestinal, and possibly other organ damage, was reduced by shock resuscitation with HbV.

These data show that significant covert damage to the intestine is present in the alb group despite seemingly adequate systemic hemodynamics. This was because of the deficiency of blood oxygen content despite sufficient volume. In contrast, systemic, as well as intestinal, perfusion in the HbValb group were well sustained and were comparable with the RBCalb group. Plasma TNF-α level was also effectively reduced in the

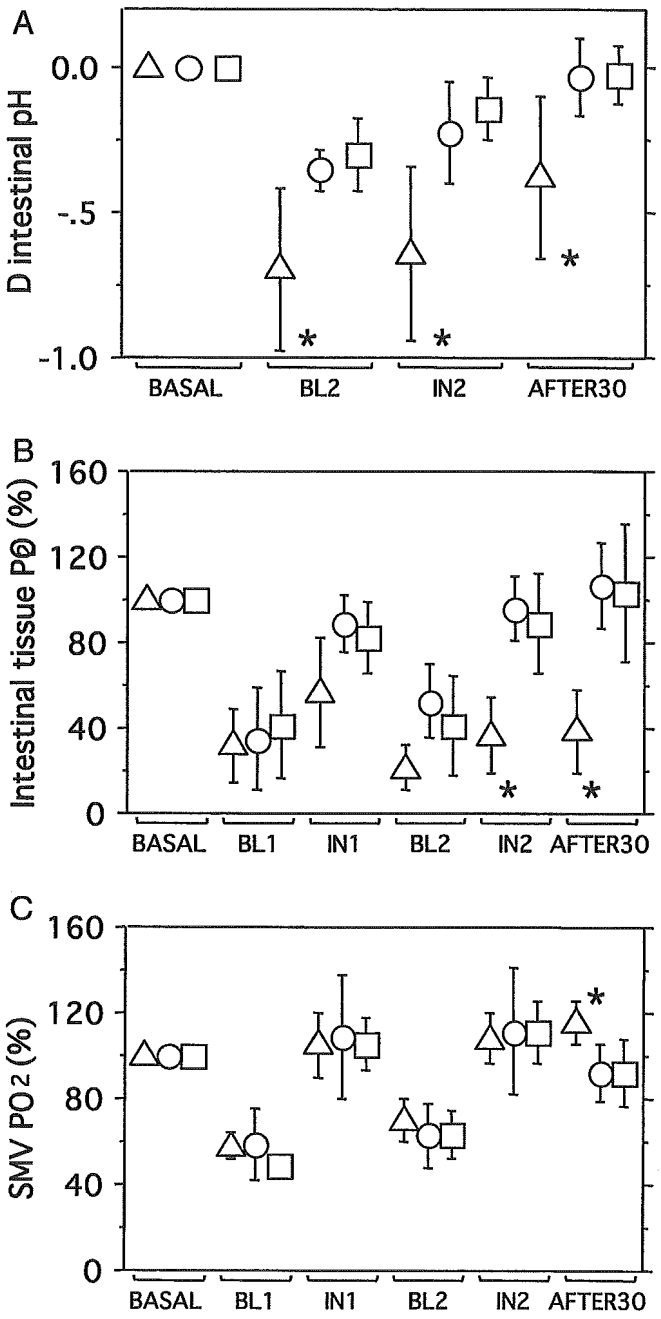

Figure 5. Parameters representing intestinal perfusion are shown as percentage changes or difference from basal values in rabbits. Time points: before bleeding (BASAL), after first bleeding (BL1), after first infusion (IN1), after second bleeding (BL2), after second infusion (IN2), and at 30 min after the second infusion (AFTER30). Triangle, alb group; circle, HbValb group; square, RBCalb group. *$p < 0.05$ *vs.* HbValb and RBCalb groups.

HbValb group, close to the RBCalb group. These data collectively indicate the proficient oxygen transporting capability of HbV and its potential efficacy in shock resuscitation. One of the powerful advantages of HbV is that its properties, such as oxygen binding and release, viscosity, and colloid osmotic pressure, can be manipulated by changing the amount of allosteric effector in HbV and the plasma expander in which to suspend HbV. We believe that currently ongoing optimization of these properties will further improve the efficacy of HbV in shock resuscitation.

Acknowledgement

This work was supported in part by a grant from the Ministry of Health, Labor and Welfare, Japan (15141201) and Grants in Aid for Scientific Research from the Ministry of Education, Japan (10470247). The authors thank BML Inc. (Kawagoe, Japan) for the cytokine measurement.

References

1. Tsuchida E: *Blood Substitutes: Present and Future Perspectives.* Amsterdam: Elsevier, 1998.
2. Chang TMS: *Blood Substitutes: Principles, Methods, Products, and Clinical Trials.* Basel: Karger, 1997.
3. Sakai H, Hara H, Yuasa M, *et al*: Molecular dimensions of Hb-based O_2 carriers determine constriction of resistance arteries and hypertension. *Am J Physiol Heart Circ Physiol* 279: H908–915, 2000.
4. Goda N, Suzuki K, Naito M, *et al*: Distribution of heme oxygenase isoforms in rat liver. Topographic basis for carbon monoxide-mediated microvascular relaxation. *J Clin Invest* 101: 604–612, 1998.
5. Takeoka S, Teramura Y, Atoji T, Tsuchida E: Effect of Hb-encapsulation with vesicles on H_2O_2 reaction and lipid peroxidation. *Bioconjug Chem* 13: 1302–1308, 2002.
6. Izumi Y, Sakai H, Hamada K, *et al*: Physiologic responses to exchange transfusion with Hemoglobin Vesicles as an artificial oxygen carrier in anesthetized rats: changes in mean arterial pressure and renal cortical oxygen tension. *Crit Care Med* 24: 1869–1873, 1996.
7. Izumi Y, Sakai H, Takeoka S, *et al*: Evaluation of the capabilities of a hemoglobin vesicle as an artificial oxygen carrier in a rat exchange transfusion model. *ASAIO J* 43: 289–297, 1997.
8. Kobayashi K, Izumi Y, Yoshizu A, *et al*: The oxygen carrying capability of hemoglobin vesicles evaluated in rat exchange transfusion models. *Artif Cells Blood Substit Immobil Biotechnol* 25: 357–366, 1997.
9. Yoshizu A, Yamahata T, Izumi Y, *et al*: The O_2 transporting capability of hemoglobin vesicle, an artificial O_2 carrier, evaluated in a rat hemorrhagic shock model. *Artif Blood* 5: 18–22, 1997.
10. Sakai H, Takeoka S, Wettstein R, Tsai AG, Intaglietta M, Tsuchida E: Systemic and microvascular responses to the hemorrhagic shock and resuscitation with Hb-vesicles. *Am J Physiol Heart Circ Physiol* 283: H1191–H1199, 2002.
11. Nelson DP, King CE, Dodd SL, Schumacker PT, Cain SM: Systemic and intestinal limits of O_2 extraction in the dog. *J Appl Physiol* 63: 387–394, 1987.
12. Carrico CJ, Meakins JL, Marshall JC, Fry D, Maier RV: Multiple-organ-failure syndrome. *Arch Surg* 121: 196–208, 1986.
13. Sori AJ, Rush BF Jr, Lysz TW, Smith S, Machiedo GW: The gut as source of sepsis after hemorrhagic shock. *Am J Surg* 155: 187–192, 1988.
14. Sakai H, Takeoka S, Park SI: Surface-modification of hemoglobin vesicles with polyethyleneglycol and effects on aggregation, viscosity, and blood flow during 90%-exchange transfusion in anesthetized rats. *Bioconjugate Chem* 8: 15–22, 1997.
15. Sakai H, Masada Y, Takeoka S, Tsuchida E: Characteristics of bovine hemoglobin for the potential source of hemoglobin-vesicles as an artificial oxygen carrier. *J Biochem* 131: 611–617, 2002.
16. Sakai H, Takeoka S, Yokohama H, Seino Y, Nishide H, Tsuchida E: Purufication of concentrated Hb using organic solvent and heat treatment. *Protein Expression Purif* 4: 563–569, 1993.
17. Tamion F, Richard V, Lyoumi S: Gut ischemia and mesenteric synthesis of inflammatory cytokines after hemorrhagic or endotoxic shock. *Am J Physiol* 273: G314–321, 1997.
18. Nordin A, Makisalo H, Mildh L, Hockerstedt K: Gut intramucosal pH as an early indicator of effectiveness of therapy for hemorrhagic shock. *Crit Care Med* 26: 1110–1117, 1998.
19. Tani T, Fujino M, Hanasawa K, Shimizu T, Endo Y, Kodama M: Bacterial translocation and tumor necrosis factor-alpha gene expression in experimental hemorrhagic shock. *Crit Care Med* 28: 3705–3709, 2000.

Available online at www.sciencedirect.com
SCIENCE DIRECT®
Biomaterials 25 (2004) 4317–4325
Biomaterials
www.elsevier.com/locate/biomaterials

Metabolism of hemoglobin-vesicles (artificial oxygen carriers) and their influence on organ functions in a rat model

Hiromi Sakai[a], Hirohisa Horinouchi[b], Yohei Masada[a], Shinji Takeoka[a], Eiji Ikeda[c], Masuhiko Takaori[d], Koichi Kobayashi[b], Eishun Tsuchida[a,*]

[a] *Advanced Research Institute for Science and Engineering, Waseda University, Okubo 3-4-1, Shinjukuku, Tokyo 169-8555, Japan*
[b] *Department of Surgery, School of Medicine, Keio University, Tokyo 160-8582, Japan*
[c] *Department of Pathology, School of Medicine, Keio University, Tokyo 160-8582, Japan*
[d] *East Takarazuka Satoh Hospital, Takarazuka 665-0873, Japan*

Received 25 August 2003; accepted 8 November 2003

Abstract

Phospholipid vesicles encapsulating Hb (Hb-vesicles: HbV) have been developed for use as artificial O_2 carriers (250 nm ϕ). As one of the safety evaluations, we analyzed the influence of HbV on the organ functions by laboratory tests of plasma on a total of 29 analytes. The HbV suspension ([Hb] = 10 g/dl) was intravenously infused into male Wistar rats (20 ml/kg; whole blood = 56 ml/kg). The blood was withdrawn at 8 h, and 1, 2, 3, and 7 days after infusion, and the plasma was ultracentrifuged to remove HbV in order to avoid its interference effect on the analytes. Enzyme concentrations, AST, ALT, ALP, and LAP showed significant, but minor changes, and did not show a sign of a deteriorative damage to the liver that was one of the main organs for the HbV entrapment and the succeeding metabolism. The amylase and lipase activities showed reversible changes, however, there was no morphological changes in pancreas. Plasma bilirubin and iron did not increase in spite of the fact that a large amount of Hb was metabolized in the macrophages. Cholesterols, phospholipids, and β-lipoprotein transiently increased showing the maximum at 1 or 2 days, and returned to the control level at 7 days. They should be derived from the membrane components of HbV that are liberated from macrophages entrapping HbV. Together with the previous report of the prompt metabolism of HbV in the reticuloendothelial system by histopathological examination, it can be concluded that HbV infusion transiently modified the values of the analytes without any irreversible damage to the corresponding organs at the bolus infusion rate of 20 ml/kg.

Keywords: Biomimetic material; Blood; Drug delivery; In vivo test; Liposome; Nanoparticle

1. Introduction

Liposomes or phospholipid vesicles have been extensively studied for the application of drug delivery system, and some are now approved for a clinical use as antifungal or anticancer therapies [1]. Another promising application is to use vesicles for encapsulating a concentrated human Hb. The resulting Hb-vesicle (HbV) can serve as an O_2 carrier with ability comparable to red blood cells (RBC) [2–4]. The advantages of the Hb-based O_2 carriers (HBOCs) are the absence of blood-type antigens and transmission of known and unknown blood-borne disease, the possibility to improve the rheological properties of blood flow according to the needs of patients, and stability for long-term storage. These characteristics will make it possible to use the HBOCs both in elective and emergency situations [5,6]. In this sense, the infusion of HBOCs becomes superior to the conventional blood transfusion that still has the potential of mismatching, infection such as HIV and hepatitis virus, and the problems of only 2–3 week preservation period. The acellular Hb modifications including polymerized Hb and polymer-conjugated Hb are now undergoing the final stages of clinical trials [7,8]. However, the cellular structure of HbV (particle diameter, ca. 250 nm) most closely mimics the characteristics of natural RBC such as the cell membrane function of physically preventing direct contact of Hb

*Corresponding author. Tel.: +81-3-5286-3120; fax: +81-3-3205-4740.
E-mail address: eishun@waseda.jp (E. Tsuchida).

0142-9612/$ - see front matter © 2003 Elsevier Ltd. All rights reserved.
doi:10.1016/j.biomaterials.2003.11.005

with the components of blood and vasculature during circulation [9]. In comparison with some acellular Hb modifications, the Hb encapsulation in vesicles suppresses hypertension induced by vasoconstriction, a theory that is suggested to be due to the high affinity of Hb with nitric oxide and carbon monoxide as vasorelaxation factors [10,11]. Moreover, the surface modification of HbV with polyethylene glycol (PEG) chains not only prolongs the circulation half-life [12] but also prevents the intervesicular aggregation and guarantees the homogeneous dispersion in the plasma phase that provides a prompt blood flow in the microcirculation and the resulting sufficient tissue oxygenation [13,14].

According to the clinical conditions HbVs are supposed to be applied for, the organism is faced with the metabolism of a large amount of both Hb and lipids, because the dose rate of HbV is significantly large. The HbV particles, as well as phospholipid vesicles, infused in the blood stream are finally captured by phagocytes in the reticuloendothelial system (RES, or mononuclear phagocytic system, MPS) [4,15]. In a previous report, we clarified by the histopathological studies of rats receiving 20 ml/kg of HbV infusion that the HbV particles were captured and metabolized within 7 days in RES mainly in the spleen and liver [16]. Transmission electron microscopy provided a clear image of the HbV particles in the phagosomes 1 day after infusion, but they disappeared within 7 days. Staining with the anti-human Hb antibody, Berlin blue, and hematoxylin/eosin showed prompt metabolism of Hb molecules with no morphological changes in the liver and spleen. The phagocytic activity decreased and then transiently increased, but tended to return to the original level. From these studies, we did not see any irreversible damage to the organs.

Serum laboratory tests are the most common diagnostic tools to monitor organ functions clinically. However, both the PEG-modified HbV particles and the chemically modified Hb solutions remained in the plasma even after usual centrifugation to remove RBC, showing significant interference effects due to the light absorption by Hb and light scattering by the particles. These interference effects hindered the accurate evaluation of plasma laboratory tests and have been regarded as a serious issue for the development of HBOCs [17,18]. However, quite recently we have clarified by an in vitro experiment that the simple removal of PEG-modified HbV as a precipitate by ultracentrifugation (50,000 *g*, 20 min) or by conventional centrifugation in the presence of a high-molecular-weight dextran diminished most of the interference effects [19]. Using this simple procedure, we aimed to evaluate the safety of HbV by the laboratory tests of plasma after bolus intravenous infusion of HbV at a rate of 20 ml/kg, the same experimental model as in the previous study [16].

2. Materials and methods

2.1. Preparation of PEG-modified HbV

The PEG-modified HbV was prepared in a sterile condition as previously reported in the literature [10, 20–22]. Hb was purified from outdated donated blood provided by the Hokkaido Red Cross Blood Center (Sapporo, Japan) and the Society of Red Cross, Japan (Tokyo, Japan). The encapsulated purified Hb (38 g/dl) contained 14.7 mM of pyridoxal 5′-phosphate (PLP, Sigma) as an allosteric effector at a molar ratio of PLP/Hb = 2.5. The lipid bilayer was composed of a mixture of 1,2-dipalmitoyl-*sn*-glycero-3-phosphatidylcholine, cholesterol, and 1,5-bis-*O*-hexadecyl-*N*-succinyl-L-glutamate at a molar ratio of 5/5/1 (Nippon Fine Chem. Co., Osaka, Japan), and 1,2-distearoyl-*sn*-glycero-3-phosphatidylethanolamine-*N*-poly(ethylene glycol) (NOF Co., Tokyo, Japan, 0.3 mol% of the total lipid). The HbCO solution and the lipid powder were mixed and stirred for 12 h at 4°C. The resulting multilamellar vesicles were extruded through membrane filters with a final filter pore size of 0.22 μm. Thus prepared PEG-modified HbV was suspended in saline at the Hb concentration of 10 g/dl, and filtrated (pore size: 0.45 μm). The physicochemical parameters of the HbV are as follows: particle diameter, 251 ± 80 nm; [Hb], 10 g/dl; [metHb], <3%; [HbCO], <2%; phospholipids, 4.0 g/dl; cholesterol, 1.7 g/dl; and oxygen affinity (P_{50}), 30 Torr. The endotoxin content was precisely measured by modified *Limulus* Amebocyte lysate gel-clotting analysis that has been developed by our group recently, and confirmed that the endotoxin content was less than 0.1 endotoxin unit/ml [23].

2.2. HbV infusion and procedure for the plasma laboratory tests

All animal studies were approved by the Animal Subject Committee of Keio University School of Medicine and performed according to NIH guidelines for the care and use of laboratory animals (NIH publication #85-23 Rev. 1985). The experiments were carried out using 40 male Wistar rats (200–210 g, Saitama Experimental Animals, Kawagoe, Japan). They were anesthetized with diethylether inhalation, and the HbV suspension was infused into the tail vein at a dose rate of 20 ml/kg ($n = 5$ for every time point). Ten rats were used to obtain the control values. All the rats were housed in cages and provided with food and water *ad libitum* in a temperature controlled room on a 12 h dark/light cycle.

After 8 h, and 1, 2, 3, and 7 days, the rats were anesthetized with 1.5% sevoflurene inhalation (Maruishi Pharm. Co., Osaka, Japan) using a vaporizer (Model

TK-4 Biomachinery, Kimura Med., Tokyo). Polyethylene tubes (PE-50, Natsume Co., Tokyo) were implanted in the carotid artery for withdrawing blood into heparinized syringes for the Hct, HbV concentration, and plasma laboratory tests. The animals were finally laparotomized and sacrificed with acute bleeding from the abdominal aorta and the liver and spleen were obtained for weight measurements. The control rats received the same procedure for the measurements.

A part of the withdrawn blood (6 ml) was centrifuged to obtain plasma which was turbid and red/brown colored due to the presence of PEG-modified HbV particles especially in the samples taken at 8 h, 1 and 2 days after infusion. The plasma was ultracentrifuged (50,000 g, 20 min) to remove the HbV particles. The obtained transparent plasma specimens were stored at −80°C until the laboratory tests at BML, Inc. (Kawagoe, Japan). The selected analytes were total protein, albumin, total bilirubin, aspartate aminotransferase (AST), alanine aminotransferase (ALT), lactate dehydrogenase (LDH), γ -glutamyltransferase (γ-GTP) alkaline phosphatase (ALP), cholinesterase (ChE), leucin amino peptidase (LAP), creatine phosphokinase (CPK), amylase, lipase, total cholesterol (Total-Chol.), cholesteryl ester (Chol.Ester), free cholesterol (Free-Chol.), HDL-cholesterol (HDL-Chol.), β-lipoprotein, triglyceride (TG), free fatty acid (FFA), phospholipids, total lipids, uric acid (UA), blood urea nitrogen (BUN), creatinine (CRE), K^+, Ca^{2+}, inorganic phosphate (IP), and Fe^{3+}. In our previous study, it was confirmed that the concentrations of the plasma components in terms of the above analytes did not change after the ultracentrifugation at 50,000 g for 20 min [19]. Since rat albumin is slightly insensitive to the bromcresol green method, the values were corrected according to Takano et al. [24].

2.3. Histopathological examination of pancreas

After sacrificing the animals by acute bleeding from the abdominal aorta, the pancreas was resected for a histopathological study. The organs were fixed in a 10% formalin neutral buffer solution (Wako Chem. Co., Tokyo) immediately after the resection, and the paraffin sections were stained with hematoxylin/eosin.

2.4. Data analysis

Differences between the control and a treatment group were analyzed using a one-way ANOVA followed by Fisher's protected least-significant difference (PLSD) test. The changes were considered statistically significant if $p<0.05$.

3. Results

All the rats receiving the bolus infusion of HbV at a dose rate of 20 ml/kg tolerated the infusion and survived until intentional sacrifice. There was no noticeable change in appearance such as piloerection.

3.1. Hct and circulation persistence of HbV

The control Hct was 42±1%, and it decreased slightly to 40±1% at 1 day after HbV infusion. The estimated Hb concentration of HbV in plasma just after infusion was about 6 g/dl, and it gradually decreased to 4.4±0.3 g/dl at 8 h, 1.9±0.2 g/dl at 1 day, 1.3±0.1 g/dl at 2 days, and 0.8±0.01 g/dl at 3 days (Fig. 1). At 7 days, HbV was not detected at all in the plasma phase.

3.2. Spleen and liver weights

The changes in the spleen and liver weights were expressed as percents of the body weight (Fig. 1). The liver weight ratio (control, 4.81±0.17%) showed a significant increase 1 day after the infusion (5.29±0.27%, $p<0.01$), and then it returned to the original level at 2 days. Spleen weight ratio significantly increased from 0.32±0.05% to 0.66±0.06% 3 days after the infusion ($p<0.01$), however, it was reduced to 0.41±0.02% at 7 days.

3.3. Plasma laboratory tests

The plasma fraction after centrifugation of the blood sample for 3 days after the HbV infusion was turbid due to the presence of PEG-modified HbV. However, ultracentrifugation of the plasma produced transparent and light-yellow plasma phase and PEG-modified HbV was precipitated at the bottom in a tube. There was no sign of the presence of Hb in the supernatant, indicating that there was no hemolysis of both RBC and HbV.

As for the analytes that reflect the liver function, the total protein (control, 5.2±0.1 g/dl) and albumin (2.46±0.06 g/dl) slightly decreased to, e.g., 4.9±0.2 and 2.11±0.10 g/dl, respectively, with statistically significant differences ($p<0.01$) for 3 days after the HbV infusion (Fig. 2). They tended to return to its original level at 7 days ($p<0.05$). AST (control, 60±7 U/l) decreased to 46±3 U/l ($p<0.05$) and returned to the original level at 7 days. ALT (control, 32±5 U/l) only slightly increased to 40±8 U/l 1 day after the HbV infusion ($p<0.01$), but it returned to its original level 2 days after the infusion. LDH (control, 150±60 U/l) did not change significantly. ALP (control, 1265±231 U/l) decreased at 2 days (812±149 U/l) and 3 days (872±98 U/l) ($p<0.01$), but it returned to the control level at 7 days. γ-GPT (control, 1.6 U/l) and LAP (31±1 U/l) showed significant but minimal reductions

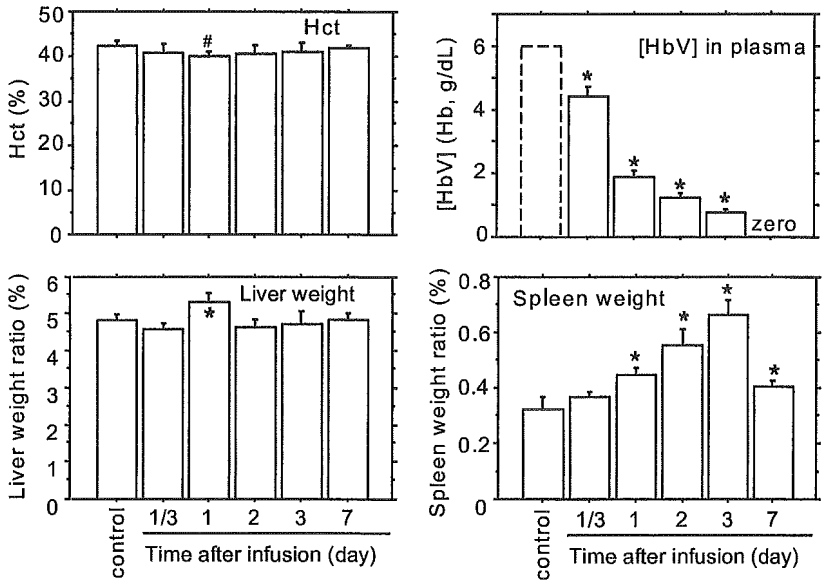

Fig. 1. Changes in hematocrit, concentration of HbV in plasma, and spleen and liver weights after infusion of HbV (20 ml/kg). The values are mean ± SD. $^{*}p<0.01$; $^{\#}p<0.05$ vs. control values. The control value of [HbV] is the estimated concentration of HbV immediately after the infusion and expressed as with a dashed line. The spleen and liver weights are expressed as the ratio to the body weight (%).

($p<0.05$). ChE (control, 76 ± 18 U/l) did not show a noticeable change. Plasma total bilirubin (≤0.1 mg/dl) and Fe^{3+} showed some reductions but were maintained at a low level for 7 days in spite of the metabolism of a large amount of Hb.

CRE (control, 0.3 mg/dl) was maintained at a low level for 7 days. BUN (control, 16 ± 3 mg/dl) showed a slight increase at 7 days (21 ± 3 mg/dl) (Fig. 3). UA (control, 0.47 ± 0.19 mg/dl) increased to 0.70 ± 0.16 mg/dl at 3 days, however, it returned to a non significant level at 7 days. Amylase (control, 1613 ± 74 U/l) significantly decreased for 3 days after the infusion ($p<0.01$), but returned to its original level at 7 days. Lipase (control, 9 ± 1 U/l) showed significant increases ($p<0.01$) after the HbV infusion, and it tended to decrease after 3 days, and was reduced to a non-significant level at 7 days. CPK (control, 304 ± 116 U/l) decreased at 7 days ($p<0.05$), but did not show a noticeable increase during the experiment. As for the electrolyte concentrations, K^{+}, Ca^{2+}, and IP did not show any significant changes.

The most consistent changes were seen in the lipid components (Fig. 4). Total-Chol. (control, 73 ± 7 mg/dl), Free-Chol. (18 ± 2 mg/dl), Chol.Ester (59 ± 8 mg/dl), and HDL-Chol. (32 ± 4 mg/dl) showed significant increases and maximum values at 2 days ($p<0.01$). Free-Chol. increased to 39 ± 4 mg/dl, about twice the control value. However, it tended to decrease at 3 days, and returned to its control level at 7 days. β-Lipoprotein (control, 110 ± 42 mg/dl) slightly increased at 1 day (160 ± 33 mg/dl), but returned to its original level at 3 days. TG (control, 64.4 mg/dl) significantly decreased to 12.4 mg/dl at 2 days ($p<0.01$), but tended to increase to its original level at 7 days. Phospholipid (control, 132 ± 8 mg/dl) significantly increased to 150 ± 9 mg/dl at 1 day ($p<0.01$), and then returned to the original level at 3 days.

3.4. Histopathological examination of pancreas

The histology of pancreatic tissue 2 days after the infusion of HbV is shown in Fig. 5. There was no significant morphological change in spite of the increment of the pancreatic lipase activity.

4. Discussion

The clinical indications for the use of the HbV suspension as an artificial O_2 carrying fluid are estimated to be mainly preoperative or perioperative hemodilution, or resuscitation from hemorrhagic shock in emergency situations [25], both of which result in exchanging more than 20% of the original blood with the HbV suspension. Thus, the dose amount is extremely greater than that of stealth liposomes for drug delivery systems. HbV particles in the blood stream are finally captured by RES in the same manner as the conventional phospholipid vesicles [15]. In a previous study, we confirmed by the histopathological examination in a rat model that HbV particles were captured in the phagosomes of liver Kupffer cells and spleen macrophages without tissue damage, and they had completely disappeared within 7 days [16]. The transient splenomegaly and hepatomegaly in Fig. 1 seemed associated with the entrapment of HbV. The total weight change of

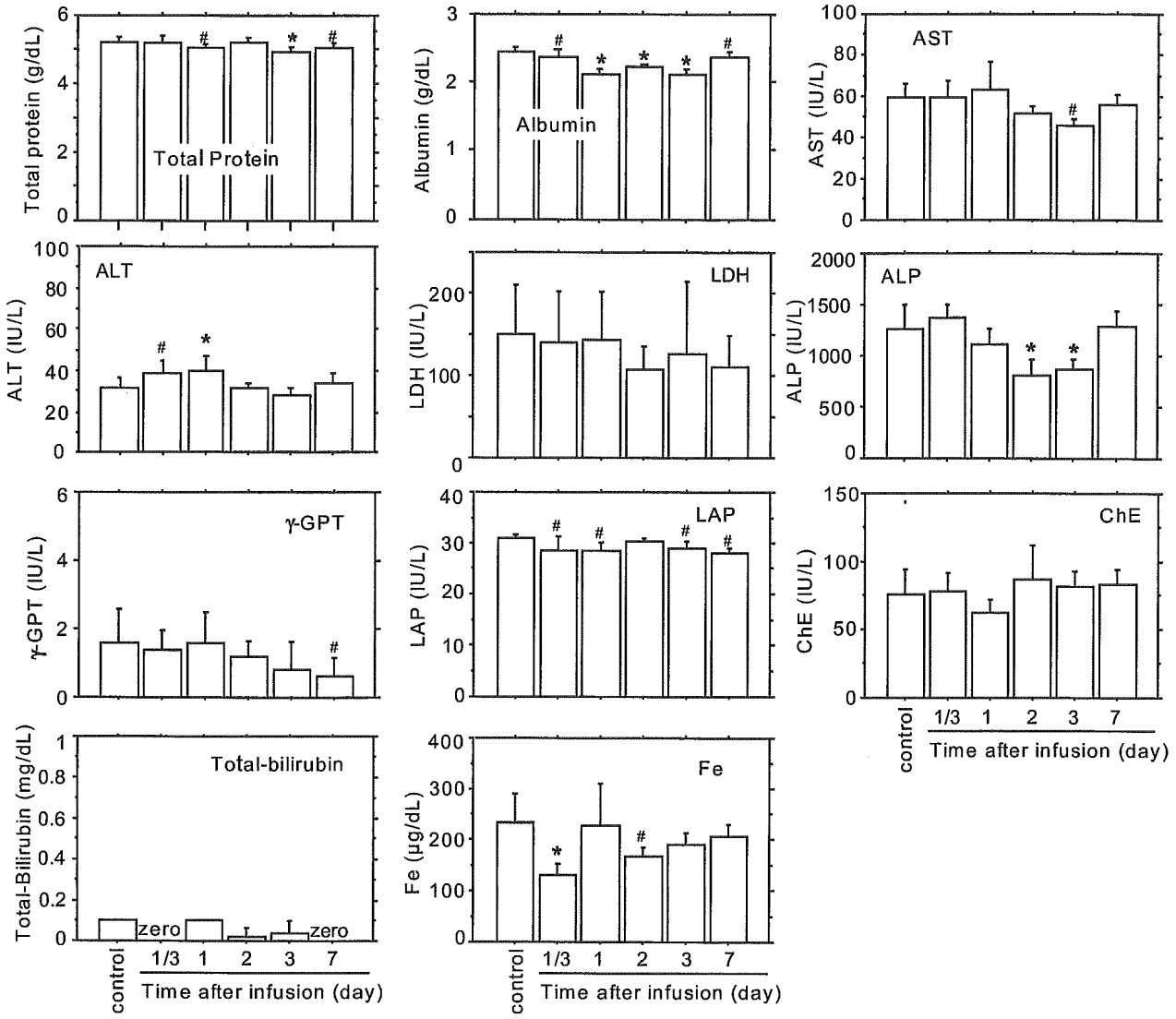

Fig. 2. Plasma laboratory tests representing the liver function and metabolism of Hb after infusion of HbV (20 ml/kg). The values are mean ± SD. $^{*}p<0.01$; $^{\#}p<0.05$ vs. control values. Abbreviations: aspartate aminotransferase (AST), alanine aminotransferase (ALT), lactate dehydrogenase (LDH), γ-glutamyltransferase (γ-GTP) alkaline phosphatase (ALP), leucin amino peptidase (LAP), cholinesterase (ChE).

these organs is 0.8% of the body weight (1600 mg for 200 g body weight), which should correspond to not only the accumulated HbV (635 mg for 20 ml/kg) but also to the increased amount of phagocytic or parenchymal cells and/or RBC. The organ weight ratios tended to return to their original levels as HbV disappeared from the blood stream, and there was no deteriorative sign of morphological change in the main organs such as the liver, spleen, lung, kidney, and heart. To confirm the safety more in detail, we analyzed for the first time, the plasma laboratory tests on 29 analytes without any interference effect of the PEG-modified HbV simply by removing it from plasma by ultracentrifugation [19].

Our results indicated no irreversible sign of organ damage after the bolus infusion of HbV at a dose rate of 20 ml/kg (cf. whole blood = 56 ml/kg). Especially, liver is one of the main organs of the trapping and metabolism of HbV. However, we did not see an increase in the physiological meaning of the parameters representing the liver function. As for the parameters representing the renal function, there were slight changes in CRE, BUN, and UA without any physiological meanings. CPK did not significantly change, indicating that the intactness of the cardiac function and skeletal muscular function should be preserved.

Amylase and lipase that represent pancreatic function showed slight changes. The amylase activity slightly decreased while the lipase activity significantly increased from 9 ± 1 IU/l at control to 30 ± 9 IU/l at 2 days. The lipase activity was measured by an enzymatic method that was specific for pancreatic lipase. Therefore, the increment should not be attributed to the hepatic or

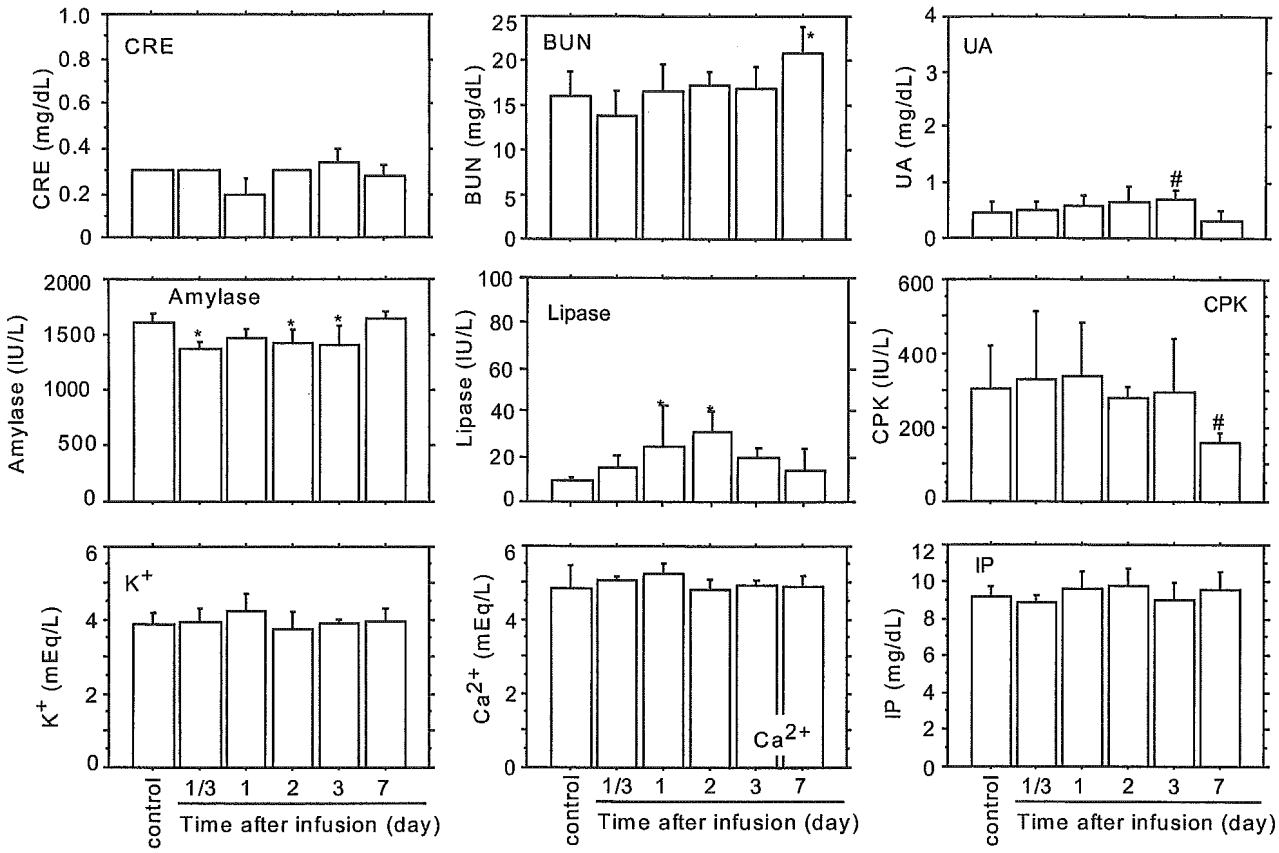

Fig. 3. Plasma laboratory tests representing renal, pancreatic and myocardial function, and electrolytes after infusion of HbV (20 ml/kg). The values are mean±SD. $^{*}p<0.01$; $^{\#}p<0.05$ vs. control values. Abbreviations: creatinine (CRE), blood urea nitrogen (BUN), uric acid (UA), creatine phosphokinase (CPK), inorganic phosphate (IP).

lipoprotein lipase. However, this level of increment was significantly smaller than the reported value for the Wistar rats of pancreatitis. Hofbauer et al. [26] reported that acute necrotising pancreatitis increased lipase activity from 10 to 475–5430 IU/l. It was reported that the injection of liposome amphotericin B raised the serum lipase activity, and one possible reason was speculated to be the enzyme induction in the pancreas by the presence of a large amount of lipids from the liposomes [27], because pancreatic lipase hydrolyze not only TG but also phosphatidylcholine [28]. This speculation was also supported by our results that the profiles of the transient increases in the lipid components coincided with that of lipase, but not with amylase. The cause of this modification is not clear at the present time. Histopathological analysis showed no significant pathological change in the pancreas. However, the pancreatic function should carefully be monitored in the ongoing safety studies.

Significant and consistent increases were seen in the lipid components with maximum at 1 or 2 days. They should be derived from the HbV particles because they contain a large amount of cholesterol (ca. 1200 mg/dl) and DPPC (1840 mg/dl) in the infused suspension ([Hb] = 10 g/dl). The gradual increases in cholesterols by 2 days after infusion and no Hb release from HbV in the plasma indicate that they should be liberated from RES after HbV are captured by RES and destroyed in the phagosomes. This is also supported by the fact that the maximum concentrations were seen at 2 days when the HbV in the plasma had mostly disappeared from the blood. It has been reported that the infused lipid components of the phospholipid vesicles are trapped in the Kupffer cells, and diacylphosphatidylcholine is metabolized and reused as a component of the cell membrane, or excreted in the bile and in the exhaled air [29–31]. Cholesterol is finally catabolized as bile acids in the parenchymal hepatocytes. There should be no direct contact of HbV and the hepatocytes because HbV is so large that it cannot diffuse across the fenestrated endothelium into the space of Disse [11]. Cholesterol from HbV should reappear in the blood mainly as lipoprotein cholesterol after entrapment in the Kupffer cells [32], and then excreted in the bile after entrapment of the corresponding lipoprotein by the hepatocytes [33]. We speculate that the main components of the lipid bilayer membrane of HbV, the phospholipids and cholesterol, would gradually be redistributed